UNIVERSIDAD
POLITECNICA
DE VALENCIA

A Burnup Credit Methodology for PWR Spent Fuel Storage Pool

Thesis submitted to the Universitat Politècnica de València in partial fulfillment of the requirements for the degree of

MASTER OF SCIENCE
In
Nuclear and Chemical Engineering

Author: Victor Faria de Castro
Advisors: Rafael Miró Herrero
Gumersindo Verdú Martín

Departamento de Ingeniería Química y Nuclear

May 2012

A Burnup Credit Methodology for PWR Spent Fuel Storage Pool

VICTOR FARIA DE CASTRO

(ABSTRACT)

In the past, criticality safety analyses for spent fuel storage and transport canisters assumed the spent fuel to be fresh (unburned) fuel with uniform isotopics corresponding to the maximum allowable enrichment. However, because this assumption ignores the decrease in reactivity as a result of irradiation, it is very conservative for fuel with significant burnup. The concept of taking credit for the reduction in reactivity due to fuel burnup is commonly referred to as *Burnup Credit*.

In this work a methodology for giving Burnup Credit in development is presented. The final goal is to obtain the loading curve that determines the region on a spent fuel storage pool in which a fuel element must be stored. Several analyses on the code were carried out with the SCALE6.1 code package, more specifically, the TRITON depletion sequence, with KENO-VI and NEWT transport codes, and CSAS6 criticality sequence, which uses KENO-VI transport code.

The methodology consists in determine the upper subcritical limit (USL) which is the limit for the k_{eff} at safety conditions. The USL was determined with a set of benchmark critical experiments available for SCALE. Once the bias and its uncertainty are determined the USL can be established and, with a conservative axial burnup profile, the loading curve can be obtained.

INDEX

FIGURES

TABLES

I. INTRODUCTION

Unirradiated reactor fuel has a well-specified nuclide composition that provides a straightforward and bounding approach to the criticality safety analysis of transport and storage casks [1]. In the past, criticality safety analyses for spent fuel storage and transport canisters assumed the spent fuel to be fresh (unburned) fuel with uniform isotopics corresponding to the maximum allowable enrichment. This fresh-fuel assumption provides a well-defined, bounding approach to the criticality safety analysis that eliminates all concerns related to the fuel operating history, thus, considerably simplifying the analysis. However, because this assumption ignores the decrease in reactivity as a result of irradiation, it is very conservative for fuel with significant burnup [2]

The concept of taking credit for the reduction in reactivity due to fuel burnup is commonly referred to as *Burnup Credit*. This reduction in reactivity that arises with fuel burnup is due to change in concentration of fissile nuclides and the production of parasitic neutron-absorbing nuclides. *Actinide-only* burnup credit refers to a methodology that considers only the two major actinides present in spent fuel: uranium and plutonium. *Fission product* burnup credit considers a number of fission products and minor actinides. *Full* burnup credit refers to a combination of actinide-only and fission product burnup credits.

For over two decades, burnup credit has been sought for the transportation, storage, and disposal of spent commercial nuclear fuel. Progress has included the issuance of the first version of U.S. Nuclear Regulatory Commission (NRC) Interim Staff Guidance 8 (ISG8) in 1999. The latest version, Revision 2, has endorsed actinide-only burnup credit and was issued in 2002. Experimental data necessary for validation of the isotopic compositions and the nuclear cross sections of fission products have not been deemed to be adequate thus far, and approval of full burnup credit, including both actinides and fission products, has been subsequently delayed [3]. Since 2004, Oak Ridge National Laboratory (ORNL) has been working on a project whose goal is to develop scientific and technical information necessary to support preparation and review of a safety evaluation for cask designs that use full burnup credit to transport PWR spent fuel. Cooperative work between ORNL, NRC, the Electric Power Research Institute (EPRI), and the U.S. Department of Energy (DOE) was established in order to execute this full burnup credit project [4]. The issuance of the ISG8 – Revision 3 was predicted to 2011 and presumably will provide recommendations for full burnup credit.

I.1   Criticality accident requirements

Criteria in matters of criticality analysis were based on the NRC regulation 10 CFR 50.68 [5] along with the guidance document [6]. When giving credit for soluble boron it is assumed the hypothesis that there is no loss in boron inside the spent fuel storage pool.

1. For PWR fuel storage pools where no soluble boron credit is taken, the criticality safety analysis will follow the condition:

a) If no credit for soluble boron is taken, the k-effective of the spent fuel storage racks loaded with fuel of the maximum fuel assembly reactivity must not exceed 0.95, at a 95 percent probability, 95 percent confidence level, if flooded with unborated water.

2. If soluble boron credit is taken, two conditions are to be analyzed:

a) If credit is taken for soluble boron, the k-effective of the spent fuel storage racks loaded with fuel of the maximum fuel assembly reactivity must not exceed 0.95, at a 95 percent probability, 95 percent confidence level, if flooded with borated water, and;

b) The k-effective must remain below 1.0 (subcritical), at a 95 percent probability, 95 percent confidence level, if flooded with unborated water.

I.2   Criticality safety analysis method and computational code

Following the recommendations of the [ISG8R2], the criticality safety analysis methods must adequately consider all the neutronic and geometric features of the storage pool. In particular, the storage racks that contain layers of neutron absorbing materials, or structural poisoned material (e.g. borated water), need detailed modeling.

ISG8R2 recommendation calls for validation of the analysis tools using measured data to determine appropriate bias and uncertainties [7]. In this work the code system SCALE6.1 was used in order to obtain fresh fuel burnup details (isotopic concentrations) using TRITON, for later use in the criticality analysis in the spent fuel storage pool, using CSAS6.

II. THE SCALE CODE SYSTEM

The SCALE code system, developed at Oak Ridge National Laboratory (ORNL) in the United States, provides a comprehensive, verified and validated, user-friendly tool set for criticality safety, reactor physics, spent fuel characterization, radiation shielding, and sensitivity and uncertainty analysis. SCALE6.1 is built on a modular design and provides a framework with 89 computational modules, including three deterministic and three Monte Carlo radiation transport solvers that are selected based on the desired solution.

As mentioned before, two main control modules of SCALE6.1 were used for the calculations: TRITON, a code for transport, depletion and sensitivity and uncertainty analysis, and CSAS6, a criticality code for calculation of the neutron multiplication factor for the system. Both of these codes prepare a resonance-corrected cross-section library for subsequent use in the KENO-VI 3-D transport code. Unless specified, all cases were run with the 44-groups ENDF/B-V master library available on SCALE package. Also, NEWT deterministic transport code was used on TRITON depletion sequence as a means to compare the TRITON transport codes in a burnup calculation.

II.1 TRITON: Transport Rigor Implemented with Time-dependent Operation for Neutronic depletion

TRITON is a multipurpose SCALE control module for transport, depletion, and sensitivity and uncertainty analysis for reactor physics applications. TRITON can be used to provide automated, problem-dependent cross-section processing followed by multigroup neutron transport calculations for one-, two-, and three-dimensional (1D, 2D, and 3D) configurations. Additionally, this functionality can be used in tandem with the ORIGEN depletion module to predict isotopic concentrations, source terms, and decay heat, as well as generate few-group homogenized cross sections for nodal core calculations. [15]

TRITON provides the capability to perform deterministic transport analysis for 1D geometry using XSDRNPM and for a wide variety of 2D arbitrary geometry configurations using NEWT. TRITON also includes Monte Carlo depletion capabilities using KENO V.a and KENO-VI. Both KENO codes offer powerful 3D geometric representations for depletion calculations. With the rigorous treatment of neutron transport available within XSDRNPM, NEWT and KENO, coupled with the accuracy of ORIGEN depletion capabilities and SCALE multigroup cross-section processing calculations, TRITON provides a rigorous first-principles approach for calculation of cross sections and isotopic depletion source terms for fuel designs.

Five cross-section processing options are supported in TRITON: (1) the CENTRM-based discrete ordinates option, (2) the CENTRM-based two-region option, (3) the CENTRM-based doubly heterogeneous option, (4) the NITAWL-based option, and (5) the BONAMI-based option. Because the first option, CENTRM-based discrete ordinates, is the most rigorous and accurate [14] it was the chosen cross-section processing tool for all the calculations in the study presented.

For this work, TRITON was used with the depletion sequences t-depl and *t6-depl*, which invokes NEWT and KENO-VI, respectively as transport model. Figure 1 shows the scheme used for the depletion calculation using NEWT, while Figure 2 shows a depletion scheme using KENO transport code.
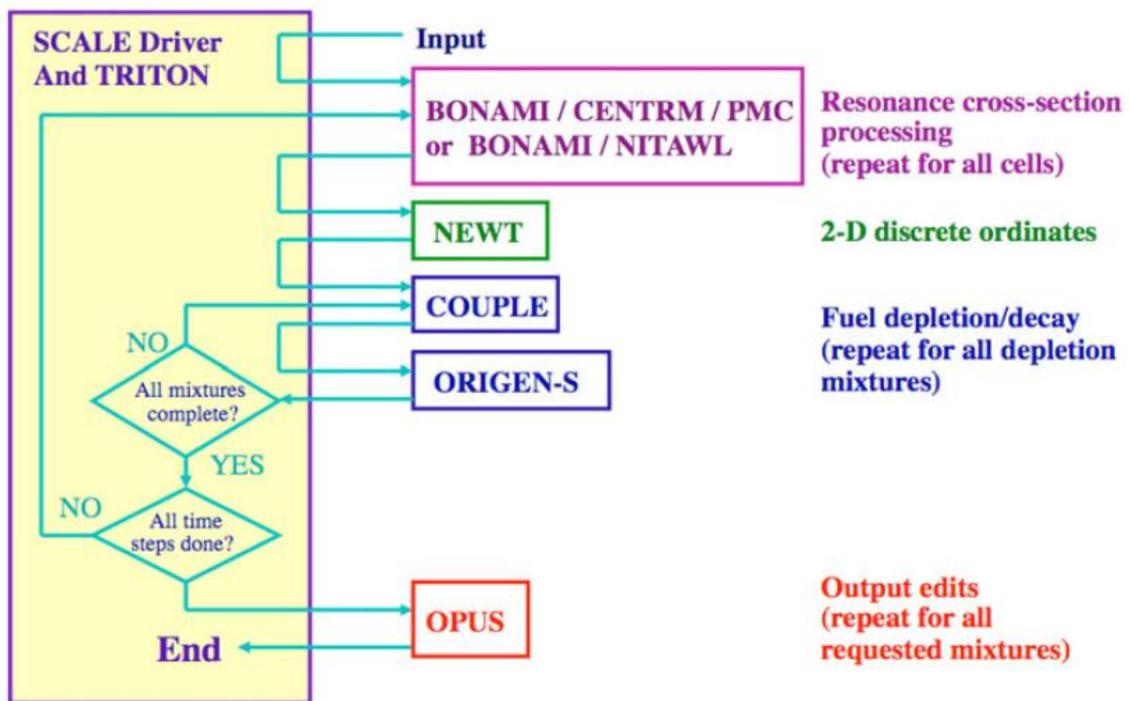
Figure 1: TRITON depletion sequence using NEWT as transport code
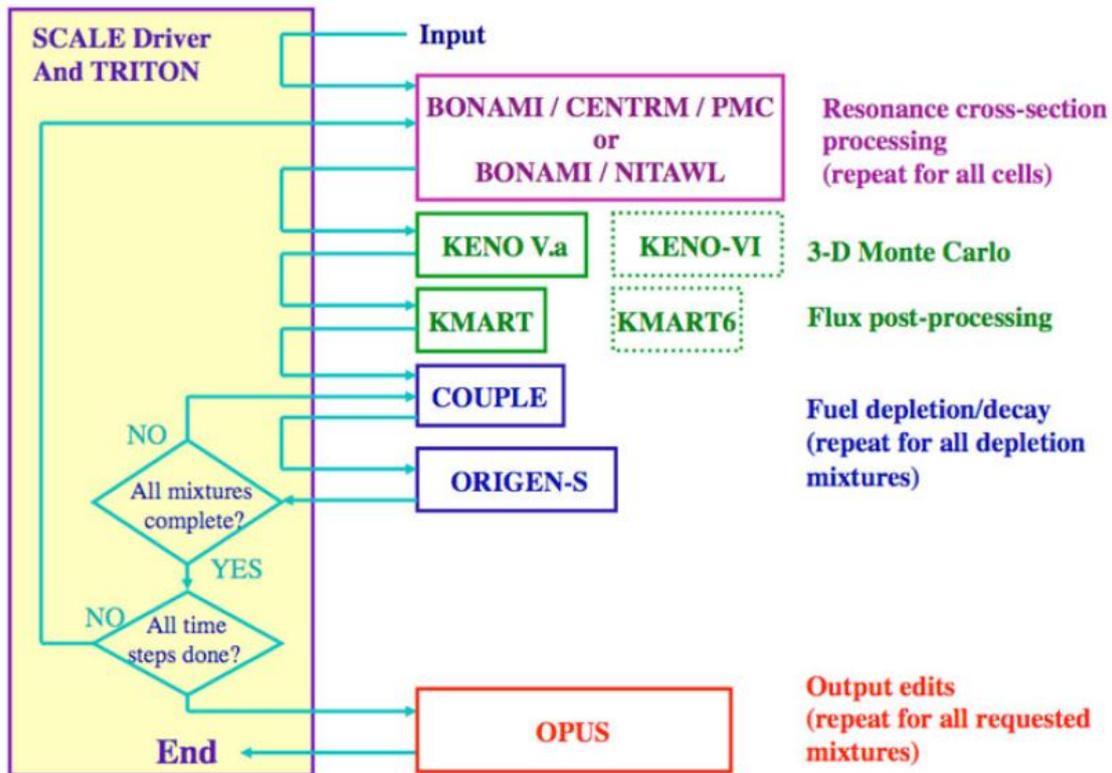
Figure 2: TRITON depletion sequence using KENO as transport code

II.2   Cross-section processing

SCALE features a material information processor for the control modules that utilize free-form input data consisting of easily visualized engineering parameters to derive and prepare input data for many of the functional modules used in SCALE.

The **M**aterial **I**nformation **P**rocessor **Lib**rary (MIPLIB) reads and checks a unified set of engineering-type data and performs the calculations that are necessary to create input data files for use by the BONAMI (**BON**darenko **AM**PX **I**nterpolator) code, and, optionally:

- CRAWDAD (**C**ode to **R**ead **A**nd **W**rite **DA**ta for **D**iscretized solution);
- NITAWL (**N**ordheim **I**ntegral **T**reatment **A**nd **W**orking **L**ibrary Production);
- CENTRM (**C**ontinuous **EN**ergy **TR**ansport **M**odule);
- PMC (**P**roduce **M**ultigroup **C**ross sections);
- CHOPS (**C**ompute **HO**mogenized **P**ointwise **S**tuff);
- CAJUN;
- WAX (**W**orking Library AJAX);
- WORKER;

- XSDRNPM (**X**-**S**ection **D**ynamics for **R**eactor **N**ucleonics with **P**etrie **M**odifications); and/or
- ICE (**I**ntermixed **C**ross Sections **E**ffortlessly) to provide a problem-dependent cross-section library.

As stated in the previous section, the CENTRM-based discrete ordinates (S_N) option was chosen in this work for cross-section processing. With this option, the Bondarenko self-shielding method is used to determine the problem-dependent multigroup cross sections in the unresolved resonance energy range. The unresolved resonance calculation is performed by the BONAMI functional module. For the resolved resonance energy range, the CENTRM functional module is used to determine the 1D pointwise (~10^5 energy groups) flux solution using an S_N method. After the BONAMI and CENTRM calculation, the PMC functional module is invoked to collapse pointwise cross sections using the CENTRM pointwise flux solution. The flux weighting provides problem-dependent multigroup cross sections in the resolved resonance range. The CENTRM S_N option also employs the SCALE functional modules CRAWDAD and WORKER to reformat data libraries to the appropriate format for BONAMI, CENTRM, and PMC.

The engineering-type data read by the Material Information Processor include the unit cell description defining the materials, dimensions, and boundary conditions of the geometry that will be used in the resonance self-shielding calculations and the flux-weighting cell calculations used in cross-section processing. Also, the user must specify the type of geometry in which the unit cell is. Because the geometry of the problem is a PWR fuel assembly, the *LATTICECELL* was used. This cell description is especially suited to large arrays of identical cells such as a fuel assembly lattice. The unit cell data are used to provide the lump shape and dimensions for resonance cross-section processing, to provide lattice corrections for cross-section processing. The unit cell data are utilized by the code to define the geometric and resonance self-shielding corrections that will be applied to the cross sections. The cell-weighted cross sections have a flux disadvantage factor applied to them. Thus, the unit cell specification plays a major role in providing accurate problem-dependent cross sections. A unit cell as used on the calculations is depicted on Figure 3.
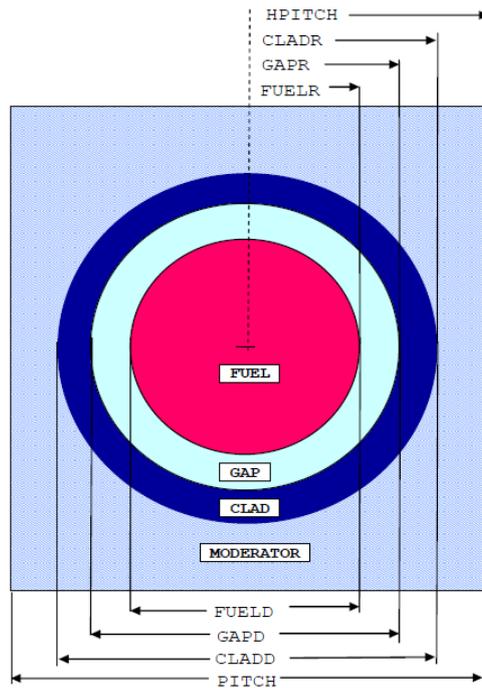
Figure 3: Unit cell used for cross-section processing

II.3   CSAS6/KENO-VI:

CASA6 is a criticality module that automatically prepares cross-sections for KENO-VI transport analysis. As TRITON cross-section processing, the CSAS6   processes SCALE cross sections using the Bondarenko method (via BONAMI) and collapsing of pointwise continuous energy cross sections using a problem dependent pointwise continuous flux (via WORKER, CENTRM, and PMC) to provide a resonance-corrected cross-section library based on the physical characteristics of the problem being analyzed. The codes utilized in CSAS6 start with an AMPX master format cross-section library and generate a self-shielded, group-averaged library applicable to the specific problem configuration. These cross sections are then used in the KENO-VI Monte Carlo code to determine the effective neutron multiplication factor (k_{eff}).

KENO-VI is a Monte Carlo transport code whose primary purpose is to determine k-effective. Other calculated quantities include lifetime, generation time, energy-dependent leakages, energy- and region-dependent absorptions, fissions, flux densities, and fission densities. It uses the SCALE Generalized Geometry Package (SGGP) which contains a much larger set of geometrical bodies, including cuboids, cylinders, spheres, cones, dodecahedrons, elliptical cylinders, ellipsoids, hoppers, parallelepipeds, planes, rhomboids, and wedges. The code's flexibility is increased by allowing the following features: intersecting geometry regions; hexagonal, dodecahedral, and cuboidal arrays; bodies and holes rotated to any angle

and translated to any position; and a specified array boundary that contains only that portion of the array located inside the boundary.

SCALE also provides a visualization tool for KENO, called KENO3D, which provides the user a means to obtain a visual model of the geometry and all the materials present in the model.

II.4 NEWT

NEWT (**N**ew **E**SC-based **W**eighting **T**ransport code) is a two-dimensional (2-D) discrete-ordinates transport code developed based on the Extended Step Characteristic (ESC) approach for spatial discretization on an arbitrary mesh structure. The ESC approach was developed to obtain a discrete-ordinates solution in complicated geometries to handle the needs of irregular configurations. Deterministic solutions to the transport equation generally calculate a solution in terms of the particle flux; the flux is the product of particle density and speed and is a useful quantity in the determination of reaction rates that characterize nuclear systems. NEWT provides multiple capabilities that can potentially be used in a wide variety of application areas.

These include 2-D eigenvalue calculations, forward and adjoint flux solutions, multigroup flux spectrum calculations, and material-weighted cross-section collapse. NEWT provides significant functionality to support lattice-physics calculations, including assembly cross-section homogenization and collapse, calculation of assembly discontinuity factors (for internal and reflected assemblies), diffusion coefficients, pin powers, and group form factors. Used as part of the TRITON depletion sequence, NEWT provides spatial fluxes, weighted multigroup cross sections, and power distributions used for multi-material depletion calculations and coupled depletion and branch calculations needed for latticephysics analysis.

II.5 ORIGEN-S

The ORIGEN (Oak Ridge Isotope Generation) code1 was developed at Oak Ridge National Laboratory (ORNL) to calculate nuclide compositions and radioactivity of fission products, activation products, and products of heavy metal transmutation. ORIGEN analyzes the full isotopic transition matrix through application of the matrix exponential method to solve the rate equations that describe the nuclide generation, depletion, and decay processes. ORIGEN-S has the ability to utilize problem-dependent multigroup cross-sections and energy-dependent fission product yields.

The libraries include nuclear data for 2226 nuclides produced by neutron activation, fission, and decay. All decay data are based on ENDF/B-VII. The multigroup cross-section data are developed from the JEFF-3.0/A neutron activation file containing cross-section data for 774 target nuclides and 23 different reaction types. In addition, energy-dependent fission product yields from ENDF/B-VII are included for 30 fissionable nuclides.

The ability to couple ORIGEN-S with cross sections developed from transport calculations is automated in the TRITON depletion sequence of SCALE. In the SCALE code system, multigroup cross-section data are available from ENDF/B-V, -VI, and -VII files. These cross sections are processed to account for the resonance self-shielding of the particular configuration specified by the user. Then they are collapsed to one group using the neutron flux spectrum determined from the transport code analysis and applied directly in the ORIGEN-S depletion calculation.

Nuclear data are stored in a binary format library developed for ORIGEN-S that contains all radioactive decay data and neutron cross sections required to solve the transmutation and decay equations. The data are stored in the library as a compressed transition matrix that can be used directly by the code. Cross sections are stored as average one-group values that have been obtained by weighting multigroup eutron cross sections. Infinite dilution cross sections for ORIGEN-S are available in multigroup format, which were obtained based on JEFF-3.0/A libraries. Alternatively, self-shielded cross sections can be accessed from any of the ENDF/B-based data libraries available in SCALE.

SCALE6.1 package also provides a utility module, called OPUS, which produces a condensed output file and plot data from output generated by the ORIGEN-S code that computes reactor fuel depletion, activation and fission- product buildup, and the associated photon and neutron source spectra.

III. CRITICALITY ANALYSIS VALIDATION

III.1 Introduction

Like mentioned before, the code CSAS6 was used for the criticality analysis, which applies the Monte Carlo transport code KENO-VI.

The criticality safety analysis was carried out using the 44-groups ENDF/B-V available in the SCALE package. The KENO-VI calculations simulated 805 generations, with 600 neutron histories per generation, and skipped the first 5 generations before averaging; thus, each calculated k_{ef} values is based on 480000 neutron histories.

III.2 The upper subcritical superior limit (USL)

For a given subcritical configuration, confidence that the system neutron multiplication factor guarantee the subcriticality of the system is necessary. This implies that an acceptable margin based on biases and uncertainties to be determined.

The USL is defined as the maximum value k_{ef} can assume, under conservative hypothesis, for the system to be consider subcritical, that is:

$$k_s + \Delta k_s \leq k_a = USL = k_c - \delta k_c - \Delta k_m - \Delta k_{BU} \qquad (1)$$

k_s –   System effective multiplication factor obtained by simulation

Δk_s –   Statistical uncertainties. Includes calculation and design uncertainties

k_c –   Average of the effective multiplication factors obtained from benchmarks experiments, using a particular calculation method.

δk_c –   Uncertainty of the benchmark experiments. Must include not only the uncertainty of these experiments, but the uncertainty on the bias, that results from extrapolation of these experiments to the range of the parameters associated to the design of the spent fuel storage pool.

Δk_m –   Subcriticality margin under operational limitations (usually $\Delta k_m = 0.05$)

Δk_{BU} –   Uncertainty to be considered when burnup credit is taken. Includes the uncertainties associated to the burnup calculations used to obtain the isotopic concentrations

To obtain the USL, the bias $\beta = (1 - k_c)$ must be determined. The benchmark sets BORON and VALSCALE were used in order to calculate this bias. These sets of critical experiments used as benchmarks are considered representative for the composition, configuration and nuclear features of the system.

The results for these benchmarks calculations are represented in the Table 1, where N is the number of experiments and δk_c, is the uncertainty in the bias $\beta = (1 - k_c)$.

Table 1: Benchmark calculations for VALSCALE and BORON sets

Experiment	N	k_c	δk_c
VALSCALE	79	1.00035	0.0172691
BORON	8	0.99426	0.0059682

For the standard experiments set for validation of the SCALE code, VALSCALE, the values for β^{VS} y $\Delta\beta^{VS}$ are obtained:

$$\beta^{VS} = 1 - k_c^{VS} = 1 - 1.00035 = -0.00035 \quad \Delta\beta^{VS} = \delta k_c^{VS} = 0.0172691 \quad\quad (2)$$

$$USL^{VS} = 1 - \Delta\beta^{VS} = 1 - 0.0172691 = 0.9827309 \quad \text{for } \beta^{VS} < 0$$

Although the reference [8] implies the values of the USL take into account the values of the bias, negative or positive, in this study, in order to be conservative, the negative bias is discarded.

For the experiments set that contain boron, BORON, the values for β^{VS} y $\Delta\beta^{VS}$ are obtained:

$$\beta^{B} = 1 - k_c^{B} = 1 - 0.99426 = 0.00574 \quad\quad \Delta\beta^{B} = \delta k_c^{B} = 0.0059682 \quad\quad (3)$$

$$USL^{B} = 1 - \beta^{B} - \Delta\beta^{B} = 1 - 0.00574 - 0.0059682 = 0.9882918 \quad \text{for } \beta^{B} > 0$$

The VALSCALE set provide the most conservative bias and uncertainty, so it will be the choice set for establishing the USL, which is the safety limit to determine when a storage pool is safe in terms of criticality.

Further analysis of the results should give more statistical data so as to obtain the USL based not only on the uncertainties provided by the SCALE6.1 code, but the statistical confidence interval accordingly to the Spanish norm UNE [9] and [5].

IV. BURNUP CREDIT METHODOLOGY IN A PWR POWER PLANT

IV.1   Introduction

In the storage pool of the studied PWR, two regions are differentiated: region I, which is the oldest, with a greater separation between element racks; and region II, with elements with a burnup degree and greater enrichment. The application of this methodology will focus on the acquisition of a criterion, which will decide the most suitable region for the safe storage of combustible material.

Initially, the spent fuel storage pool was formed by the racks in region I. Due to the lack of storage space for combustible materials, the pool was later equipped with new steel racks with a greater content of boron and of a different design, to allow the storage of a greater number of materials.

Region I can store both new and used combustible materials. Each storage position is equipped with a neutron-absorbing canal, made of bored steel with content in minimum weight of natural boron 1.6 wt%.

Region II only permits the storage of used combustible materials, with a maximum initial enrichment of 4.5 wt% in ^{235}U. These racks are made of bored steel with content in minimum weight of natural boron at 1.7 wt%.

Region II only permits the storage of combustible materials that have reached a certain level of average burnup, depending on the initial enrichment.

IV.2   Characteristics of Region II for fuel storage

The distribution of the fuel *racks* of region II, as well as that of region I, is shown in Figure 4..

Region II racks can hold spent combustible materials. The pool is equipped with neutron-absorbing vessels, made of stainless steel poisoned by at least 1.7 wt% of natural boron, in a chessboard-like configuration.

Figure 4: Region I and II of the spent fuel storage pool
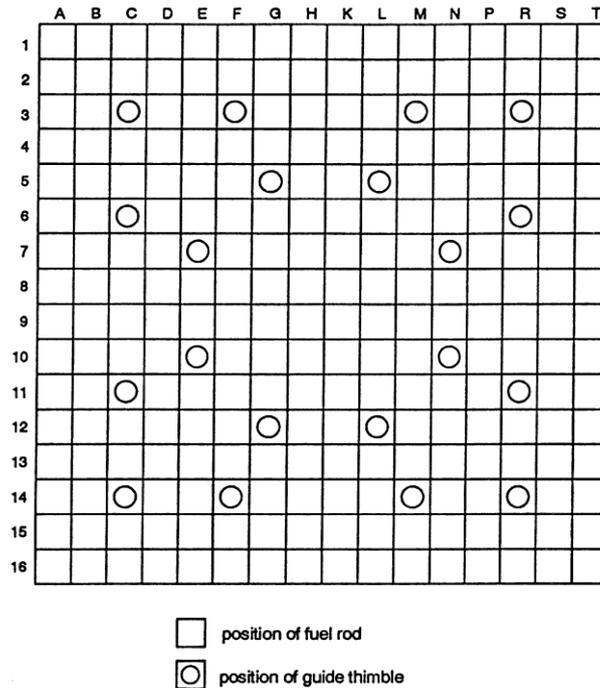
Figure 5: Guide tubes distribution on a fuel element

IV.3 Characteristics of the fuel element

The configuration of the fuel elements in the present paper is shown in Figure 5, whereas the characteristics and dimensions are given in Table 2.

Table 2: Characteristics of a fuel element in region II

Reticule	16 x 16
Number of fuel pins	*236*
Number of guide tubes	*20*
Pin pitch	*14.3 mm*
Diameter of the fuel pellets	*9.11 mm*
External diameter of the pin	*10.75 mm*
Cladding thickness	*0.725 mm*
Cladding material	*Zircaloy*
External diameter of the guide tube	*13.8 $\pm$ 0.03 mm*
Internal diameter of the guide tube	*12.4 mm*
Material of the guide tube	*Zircaloy*
Mass of uranium by fuel element	*473.2 kg $\pm$ 2%*
Active length	*3400 $\pm$ 15 mm*

IV.4 Geometric model of Region II of the fuel element pool

The fuel element pool can be modelled from a **basic,** or **reference, cell**, with boundary conditions of specular reflection on the XYZ axes, except for the case of axial burnup credit, where the reflection will exclusively be on axes X and Y (Figure 6).
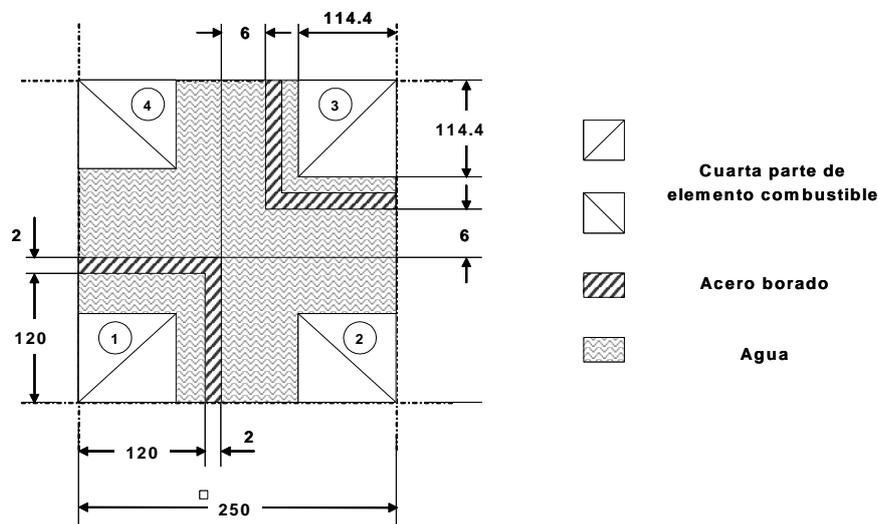
Figure 6: Outline of the reference cell model

In Table 3 the most important data for the modelling of the reference cell and that of the uranium oxide pin is shown.

Table 3: Data of cell and fuel pins

Data	Description	Value	Reference
1	Number of pins by element	236	KWU BT33-94-E065b
2	Number of guide tubes by element	20	KWU BT33-94-E065b
3	Diameter of the pellet (*cm*)	0.911	BT51-33-71331 BT41-33-72309
4	Radius of the pellet (*cm*) (3)/2	0.4555	Calculation
5	External diameter of the clad (*cm*)	1.075	BT51-33-71331
6	External radius of the clad (*cm*) (5)/2	0.5375	Calculation
7	Internal radius of the clad	0.93	BT51-33-71331
8	Internal radius of the clad (7)/2	0.465	Calculation
9	Width of the clad (*cm*) (6)-(8)	0.0725	Calculation
10	Thickness of the gap (*cm*) (8)-(4)	0.0095	Calculation
11	Active length of the element (*cm*)	340	BT41-33-72309 BT-51-33-71331
12	Maximum active length of the element (*cm*)	341.5	Calculation
13	Maximum active length of the element (*cm*)	384.5	BT-51-33-71331
14	Material of the clad	Zircaloy-4	Department of Mechanical and Materials Engineering
15	Maximum effective density of the pellets (*g/cc*)	10.5156	Calculation
16	Pin pitch (*cm*)	1.43	BT51-33-71331
17	Width of the fuel element (*16 x pin pitch*) (*cm*)	16*1.43 = 28.8	Calculation

The effective fuel pellet density is the density of the pellets averaged on:

        ❑   The pellet cells

        ❑   The active length of the fuel pins

        ❑   The number of fuel pins by fuel element

The contribution of the fuel cells can be obtained from the mass of uranium per fuel element, as specified in table 2, since this mass depends on the density of the pellet, the pellet cell, and the active length. Therefore, when considering the core fabrication tolerances specified in the previous table, the maximum possible effective density of the pellets is obtained:

$$\text{Máx}\left[(\rho_{ef})\right] = \frac{\text{Máx}\left(M_U\right)}{N_{FR}\,\pi\left(\dfrac{d}{2}\right)^2\text{Mín}\left(L_A\right)} \cdot \frac{\mu_{UO_2}}{\mu_U} = 10.5156 \; gr/cm^3$$

Max(M$_U$) = maximum mass of uranium per fuel element (473.2 *kg* + 2%)

N$_{FR}$ = number of fuel rods per fuel element (*N$_{FR}$* = 236) **(1)**

d = Diameter of the pellet (9.11 mm) **(2)**

Min(L$_A$) = minimum active length of the fuel pins (3385 mm) **(10)-15 mm**

μ_{UO2} = molecular mass of UO$_2$ (270)

μ_U = atomic mass of uranium (238)

The composition in volume of the Zircaloy-4 can be seen in Table 4. To obtain this, the values of the weight fractions of the constitutive elements were used: Zr (0.983), Sn (0.013), Fe (0.002), Cr (0.001) and O (0.0012), of the mixture density (~6.56 g/cc) and the densities of each compound Zr = 6.4 g/cc; Sn = 7.31 g/cc; Fe = 7.86 g/cc; Cr = 7.20 g/cc; O = 1.0 g/cc; according to the expression:

$$\text{Volume fraction} = \frac{(\text{Weight fraction} \cdot \text{Mixture density})}{\text{Density of compound}}$$

.

Table 4: Composition (% in volume) of Zircaloy-4

Element	% in volume
Zr	97.785
Sn	1.170
Fe	0.167
Cr	0.091
O	0.787

The guide tube is used to control the power and the neutron flux during the burnup of the element inside the reactor. In Table 5 can be seen the most significant data for the modelling of the guide tube.

Table 5: Geometric data of the guide tube

Data	Description	Value	Reference
1	Number of guide tubes by fuel element	20	KWU BT33-94-E065b
2	Internal diameter of the guide tube (cm)	1.24	BT51-33-71331
3	Internal radius of the guide tube (cm) (2)/2	0.62	Calculation
4	External diameter of the guide tube (cm)	1.38	BT51-33-71331
5	External radius of the guide tube (cm) (4)/2	0.69	Calculation
6	Pin Pitch (cm)	1.43	BT51-33-71331
7	Material of the guide tube	Zircaloy-4	Department of Mechanical and Materials Engineering

The reference cell is the basic unit that defines the spent fuel pool of region II. The data and their origin reference for the modelling of the reference cell are given in Table 6.

Table 6: Data of the reference cell

Data	Description	Value	Reference
1	Fuel *Pitch* (*mm*)	250 ± 0.5	KWU BT33-94-E065b
2	Internal length of the neutron-absorbing canal (*mm*)	240 ± 1	KWU BT33-94-E065b
3	Wall thickness of the absorbing canal (*mm*)	2	KWU BT33-94-E065b
4	Temperature (except when otherwise indicated) (*ºC*)	4	Hypothesis Design criterion
5	Material of the absorbing canal	Borated steel	KWU BT33-94-E065b
6	Density of the absorbing canal (*g/cc*)	7.647	KWU BT33-94-E065b
7	Number of neutron generations	805	Hypothesis Design criterion
8	Number of neutrons per generation	600	Hypothesis Design criterion
9	Number of rejected generations	3	Hypothesis Design criterion

V. BURNUP ISOTOPES

V.1 Determination of actinides and fission products

Although ORIGEN-S can track over 2000 nuclides, this much detail is not necessary, because a great number of those nuclides decay very rapidly, while others are not presented in sufficient amounts as to be considered important in the k_{ef} calculations. The following criteria are recommended by DeHart [10] and are considered adequate for the nuclides to be considered in the analysis.

1. Those nuclides that contribute significantly to the absorption of thermal neutrons in spent fuel are to be included;

2. All fissile nuclides are to be included;

3. Nuclides must be fixed in the fuel matrix (i.e., no credit taken for volatile elements); and

4. The predicted concentrations of selected nuclides in spent fuel must be verifiable by comparison with chemical assay measurements.

Criterion 2 requires [235]U, [239]Pu y el [241]Pu to be included in the actinide set. Moreover the guide [6] clearly express that [135]Xe must not be included.

Table 7 shows the selected nuclides for the analysis. These nuclides are part of a TRITON set that adds trace quantities of specific nuclides for the ORIGEN-S calculations. As previously stated, the parameter *ADDNUX* was fixed to the value *ADDNUX=2* from which, apart from the [135]Xe, all nuclides added were used for the criticality analysis of the storage pool.

Table 7: Selected nuclides in the burnup calculations

Actinides	^{234}U, ^{235}U, ^{236}U, ^{238}U, ^{237}Np, ^{238}Pu, ^{239}Pu, ^{240}Pu, ^{241}Pu, ^{242}Pu, ^{241}Am, ^{243}Am, ^{242}Cm, ^{243}Cm, ^{244}Cm
Fission Products	^{1}H, ^{10}B, ^{11}B, ^{14}N, ^{16}O, ^{83}Kr, ^{93}Nb, ^{94}Zr, ^{95}Mo, ^{99}Tc, ^{103}Rh, ^{105}Rh, ^{106}Ru, ^{109}Ag, ^{126}Sn, ^{135}I, ^{131}Xe, ^{133}Cs, ^{134}Cs, ^{135}Cs, ^{137}Cs, ^{143}Pr, ^{144}Ce, ^{143}Nd, ^{145}Nd, ^{146}Nd, ^{147}Nd, ^{147}Pm, ^{148}Pm, ^{149}Pm, ^{148}Nd, ^{147}Sm, ^{149}Sm, ^{150}Sm, ^{151}Sm, ^{152}Sm, ^{151}Eu, ^{153}Eu, ^{154}Eu, ^{155}Eu, ^{152}Gd, ^{154}Gd, ^{155}Gd, ^{156}Gd, ^{157}Gd, ^{158}Gd, ^{160}Gd, ^{91}Zr, ^{93}Zr, ^{95}Zr, ^{96}Zr, ^{95}Nb, ^{97}Mo, ^{98}Mo, ^{99}Mo, ^{100}Mo, ^{101}Ru, ^{102}Ru, ^{103}Ru, ^{104}Ru, ^{105}Pd, ^{107}Pd, ^{108}Pd, ^{113}Cd, ^{115}In, ^{127}I, ^{129}I, ^{133}Xe, ^{139}La, ^{140}Ba, ^{141}Ce, ^{142}Ce, ^{143}Ce, ^{141}Pr, ^{144}Nd, ^{153}Sm, ^{156}Eu

Although [6] points that all fission products, but ^{135}Xe can be used, a total of 15 actinides and 77 fission products were selected.

VI. INFLUENCE OF THE OPERATION PARAMETERS ON ISOTOPE CALCULATIONS

VI.1   Introduction

The isotope inventory of a fuel element depends on its burnup history: that is, not only on the operational cycles of the reactor, but also on the specific power at which the fuel element has been operating on the nucleus, as well as the thermal-hydraulic parameters of the operation. This implies that each burnup element has its own unique history, which differs from the rest of the elements [11].

Thus, the follow-up of the history of the specific operation of each fuel element is unfeasible for the proposals of design and security analysis, and, therefore, it is necessary to identify a simpler operation history, which is conservative in terms of k_{ef}.

For a better understanding of the effects of the operation history with regard to power, the effects of the **mean specific power** and the **burnup time** must be separated in the isotope inventory. In order to analyse this effect, several calculations have been carried out, using the code TRITON to obtain the isotopic distribution resulting from the element burnup, from the initial enrichment and CSAS6 for the criticality calculations performed so to obtain the k_{ef}.

VI.2   Effect of the average burnup in the burnup calculations

Three burnup groups had been evaluated: 10, 20 and 30 GWd/MTU along with three types of enrichment: 3.0, 3.6, 4.5 wt%. To be even more conservative, no cooling time was assumed. The results in terms of K_{ef} are presented in Table 8 and will serve as the case basis for the following calculations of this section.

Table 8: Basis Case

Enrichment	10 GWd/MTU	20 GWd/MTU	30 GWd/MTU
3.0%	1.03302 ± 0.00085	0.93620 ± 0.00082	0.84582 ± 0.00081
3.6%	1.08608 ± 0.00095	0.99546 ± 0.00092	0.90840 ± 0.00089
4.5%	1.14761 ± 0.00094	1.06515 ± 0.00089	0.98748 ± 0.00086

In general, the results reveal that the value calculated for k_{ef} increases as the specific power is increased. This behaviour is because the creation of fission products depends on the specific power, but not on the decay rate.

On the other hand, there are some contrasting effects. Thus, an increase in the concentration of ^{235}U is quite probable as the specific power increases, since there is an increase in the concentration of plutonium isotopes, and therefore, the fissions of ^{239}Pu and ^{241}Pu cause a decrease in the fission rates of

^{235}U, required to maintain the fixed level of power. In addition, both the ^{239}Pu and the ^{241}Pu are produced by the absorption of the ^{238}U of high-energy neutrons.

This also suggests that the hardening of the neutron spectrum, produced when operating at high specific power, also favours the production of both isotopes. A possible cause of this hardening is the poisoning effect of *Xenon* during the operation of the reactor, since its equilibrium state is proportional to the specific power.

Another possible effect is the decay of ^{241}Pu at ^{241}Am. At low levels of specific power, this decay is more important than fission, which causes the diminishing of the k_{ef}, since the ^{241}Am, is a highly absorbing nuclide.

As can be observed, there are contrasting effects. Thus, if the production of actinides predominates, the k_{ef} will be smaller at low power. If more fission products had been chosen, the opposite would have happened, that is, that the production of fission products would have predominated, and at high specific power, the k_{ef} would be smaller.

In the case considered, when eliminating most isotopes coming from fission products, the results are not conclusive. There is no a specific conservative power, which leads us to select the specific reference power for all the calculations, as the power obtained as a mean of three 365-day burnup cycles.

VI.3 Effect of burnup time-dependent variations

The isotopic distribution at the end of a fuel assembly life depends on the burnup history until it reaches said point. In this section such history, including downtimes is analyzed. The same burnup and enrichment groups from the previous sections are used. A total of seven different cases had been carried out:

Case 1: One month downtime (30 days).

| P_1 | 15 days | P_2 | 15 days | P_3 |
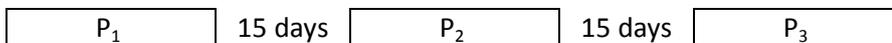
Case *2*: No downtime is assumed for the next cases.

| P_1 | P_2 | P_3 |

Case *3*: $P_1 = P_2 = 2P_3$

| P_1 | P_2 | P_3 |

Case *4*: $P_2 = 2P_1 = 2P_3$

| P_1 | P_2 | P_3 |

Case *5*: $P_1 = 2P_2 = 2P_3$

P₁		

(diagram: P₁ above, P₂ and P₃ below)

Case *6*: $P_3 = 2P_1 = 2P_2$

(diagram: P₁ and P₂ below, P₃ above)
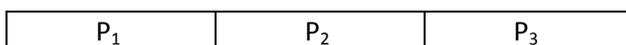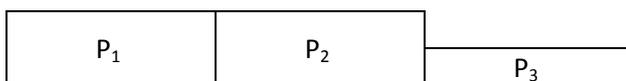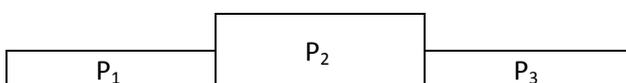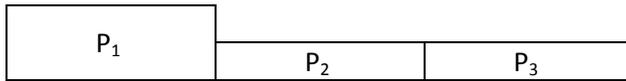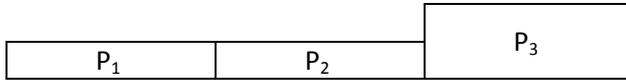
Case *7*: $P_1 = P_2 = P_3 = P_4$

(diagram: P₁, P₂, P₃, P₄)
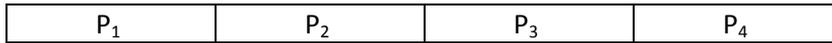
$$\sum_i P_i \big/ n_{cycles} = P_{nominal\ average}$$

Tables 9 to Table 11 show the obtained results. The most conservative values of the K_{ef} are highlighted.

Table 9: Results for burnup time-dependent variations at 3.0%

	Enrichment 3.0 wt%		
	10 GWd/MTU	20 GWd/MTU	30 GWd/MTU
Case 1	1.03403 ± 0.00093	0.94361 ± 0.00091	0.86386 ± 0.00086
Case 2	1.03536 ± 0.00094	0.94476 ± 0.00084	0.86331 ± 0.00083
Case 3	1.03596 ± 0.00092	0.94469 ± 0.00090	0.86548 ± 0.00078
Case 4	**1.03624 ± 0.00093**	0.94628 ± 0.00089	**0.86590 ± 0.00089**
Case 5	1.03456 ± 0.00086	0.94402 ± 0.00088	0.86499 ± 0.00078
Case 6	1.03416 ± 0.00087	**0.94639 ± 0.00086**	0.86427 ± 0.00085
Case 7	1.03621 ± 0.00089	0.94453 ± 0.00088	0.86537 ± 0.00085
Basis Case	1.03525 ± 0.00081	0.94421 ± 0.00064	0.86440 ± 0.00049
ΔK/K (σ)	-0.003% (0.00096)	0.073% (0.00106)	0.039% (0.00095)

Table 10: Results for burnup time-dependent variations at 3.6%

|	Enrichment 3.6 wt%		
	10 GWd/MTU	20 GWd/MTU	30 GWd/MTU
Case 1	1.08636 ± 0.00104	0.99874 ± 0.00086	**0.92297 ± 0.00079**
Case 2	1.08542 ± 0.00093	0.99941 ± 0.00107	0.92180 ± 0.00079
Case 3	**1.08693 ± 0.00093**	0.99977 ± 0.00095	0.92066 ± 0.00092
Case 4	1.08624 ± 0.00092	1.00105 ± 0.00090	0.91970 ± 0.00081
Case 5	1.08556 ± 0.00087	0.99949 ± 0.00094	0.92093 ± 0.00081
Case 6	1.08577 ± 0.00090	1.00117 ± 0.00090	0.92048 ± 0.00082
Case 7	1.08543 ± 0.00093	**1.00139 ± 0.00084**	0.92201 ± 0.00088
Basis Case	1.08578 ± 0.00077	1.00068 ± 0.00068	0.92120 ± 0.00058
ΔK/K (σ)	0.016% (0.00057)	-0.053% (0.00104)	0.002% (0.00110)

Table 11: Results for burnup time-dependent variations at 4.5%

	Enrichment 4.5 wt%		
	10 GWd/MTU	20 GWd/MTU	30 GWd/MTU
Case 1	1.14531 ± 0.00102	**1.06813 ± 0.00095**	0.99271 ± 0.00099
Case 2	1.14502 ± 0.00112	1.06641 ± 0.00089	0.99183 ± 0.00084
Case 3	1.14462 ± 0.00101	1.06695 ± 0.00094	0.99317 ± 0.00081
Case 4	**1.14576 ± 0.00092**	1.06799 ± 0.00104	0.99285 ± 0.00086
Case 5	1.14449 ± 0.00095	1.06668 ± 0.00088	0.99158 ± 0.00087
Case 6	1.14504 ± 0.00092	1.06705 ± 0.00093	0.99233 ± 0.00088
Case 7	1.14434 ± 0.00091	1.06775 ± 0.00095	**0.99429 ± 0.00093**
Basis Case	1.14482 ± 0.00091	1.06607 ± 0.00071	0.99371 ± 0.00074
ΔK/K (σ)	0.010% (0.00050)	0.114% (0.00067)	-0.104% (0.00091)

$$\frac{\Delta K}{K}(\%) = \frac{\overline{K} - K_{BASIS}}{K_{BASIS}} * 100; \quad \sigma = \sqrt{\frac{\sum_i^7 (K_i - \overline{K})^2}{6}}; \quad \overline{K} = \frac{1}{7}\sum_i^7 K_i$$

It can be concluded that, in general, when there are specific powers that are above average during the five last cycles of fuel element, higher k_{ef} are obtained, whenever the effect of the actinides is greater than that of the fission products, which is consistent with the analysis carried out in the previous section. Therefore, eliminating both effects will depend on the specific power and the burnup history.

However, when considering that 5% of the decrease in the effective multiplication constant corresponding to the burnup under study has been viewed as an unknown value, (5 % of $k_{ef\ (fresh)}$ - $k_{ef\text{-}maximum\ (spent)}$), the one closer to reality will be taken as the simple operational history. Thus, a downtime, or stopping time, between cycles, which is equal to 15 days and a final cooling time of 6.25 days (150 hours).

The specific power, in *GW* by fuel element, once the burnup time has been established within the reactor for each fuel element, has been calculated for each burnup case as

$$P = 0.482664 \left(\frac{TU}{element}\right) B \left(\frac{GWd}{TU}\right) \frac{1}{3 \, x \, 365 \; days}$$

where validity has been given to the hypothesis of three one-year cycles for each fuel element, before being discharged into the pool. The value of 0.482664 is given, since it has been assumed that a fuel element has a mass of 482.664 Kg. of Uranium.

VI.4 Sensitivity analysis with respect to operational parameters

In this section, one of the operational parameters of the basis case was perturbed, whilst the others remained fixed. The basis case parameters are as follow:

$$\overline{T}_M = 584K$$
$$\overline{T}_F = 1040K$$
$$\overline{T}_C = 618K$$
$$\overline{C}_B = 0 \, ppm$$

Fixing three of them, the other is perturbed, resulting in the following cases:

- *Case 1:* $\overline{T}_M + 100, \ \overline{T}_C + 100, \ \overline{T}_F + 50, \ \overline{C}_B$
- *Case 2:* $\overline{T}_M - 100, \ \overline{T}_C - 100, \ \overline{T}_F - 50, \ \overline{C}_B$
- *Case 3:* $\overline{T}_M, \ \overline{T}_C, \ \overline{T}_F + 100, \ \overline{C}_B$
- *Case 4:* $\overline{T}_M, \ \overline{T}_C, \ \overline{T}_F - 100, \ \overline{C}_B$
- *Case 5:* $\overline{T}_M + 50, \ \overline{T}_C + 50, \ \overline{T}_F, \ \overline{C}_B$
- *Case 6:* $\overline{T}_M - 50, \ \overline{T}_C - 50, \ \overline{T}_F, \ \overline{C}_B$
- *Case 7:* $\overline{T}_M, \ \overline{T}_C, \ \overline{T}_F, \ \overline{C}_B + 500 \, ppm$
- *Case 8:* $\overline{T}_M, \ \overline{T}_C, \ \overline{T}_F, \ \overline{C}_B + 1000 \, ppm$

The results of this analysis are presented in Table 12 to Table 15. As the previous section, the most conservative values are highlighted.

Table 12: Results for operational parameters variations at 3.0%

	Enrichment 3.0 wt%		
	10 GWd/MTU	20 GWd/MTU	30 GWd/MTU
Fuel +50°C	1.03253 ± 0.00087	0.94036 ± 0.00085	0.85745 ± 0.00078
Clad +100°C	-0.26%	-0.41%	-0.80%
Moderator +100°C			
Fuel -50°C	**1.03832 ± 0.00091**	**0.9507 ± 0.00090**	**0.87297 ± 0.00086**
Clad -100°C	0.30%	0.69%	0.99%
Moderator -100°C			
Fuel +100°C	1.03393 ± 0.00101	0.94685 ± 0.00078	0.86798 ± 0.00085
Clad = 618K	-0.13%	0.28%	0.41%
Moderator = 584K			
Fuel -100°C	1.03242 ± 0.00100	0.94279 ± 0.00083	0.86285 ± 0.00093
Clad = 618K	-0.27%	-0.15%	-0.18%
Moderator = 584K			
Fuel = 1040K	1.03136 ± 0.00095	0.94235 ± 0.00081	0.86019 ± 0.00085
Clad +50°C	-0.38%	-0.20%	-0.49%
Moderator +50°C			
Fuel = 1040K	1.03686 ± 0.00087	0.94750 ± 0.00084	0.86979 ± 0.00081
Clad -50°C	0.16%	0.35%	0.62%

Moderator -50°C			
Basis Case	1.03525 ± 0.00081	0.94421 ± 0.00064	0.86440 ± 0.00049
Power 100%	-0.0979%	0.0934%	0.0931%
Conc. Boron = 0 ppm			

Table 13: Results for operational parameters variations at 3.6%

	Enrichment 3.6 wt%		
	10 GWd/MTU	20 GWd/MTU	30 GWd/MTU
Fuel +50°C	1.08347 ± 0.00098	0.99507 ± 0.00084	0.91495 ± 0.00088
Clad +100°C	-0.21%	-0.56%	-0.68%
Moderator +100°C			
Fuel -50°C	1.08808 ± 0.00088	**1.00618 ± 0.00088**	**0.92668 ± 0.00081**
Clad -100°C	0.21%	0.55%	0.59%
Moderator -100°C			
Fuel +100°C	1.08409 ± 0.00094	1.00031 ± 0.00087	0.92410 ± 0.00082
Clad = 618K	-0.16%	-0.04%	0.31%
Moderator = 584K			
Fuel -100°C	1.08468 ± 0.00097	1.00094 ± 0.00090	0.92151 ± 0.00082
Clad = 618K	-0.10%	0.03%	0.03%
Moderator = 584K			
Fuel = 1040K	1.08536 ± 0.00093	0.99887 ± 0.00085	0.91833 ± 0.00082
Clad +50°C	-0.04%	-0.18%	-0.31%
Moderator +50°C			
Fuel = 1040K	**1.08844 ± 0.00097**	1.00414 ± 0.00104	0.92504 ± 0.00088
Clad -50°C	0.24%	0.35%	0.42%
Moderator -50°C			
Basis Case	1.08578 ± 0.00077	1.00068 ± 0.00068	0.92120 ± 0.00058
Power 100%	-0.0086%	0.0238%	0.0617%
Conc. Boron = 0 ppm			

Table 14: Results for operational parameters variations at 4.5%

	Enrichment 4.5 wt%		
	10 GWd/MTU	20 GWd/MTU	30 GWd/MTU
Fuel +50°C	1.14113 ± 0.00098	1.06310 ± 0.00096	0.99028 ± 0.00086
Clad +100°C	-0.66%	-1.25%	-1.43%
Moderator +100°C			
Fuel -50°C	1.14471 ± 0.00092	**1.06992 ± 0.00092**	**0.99618 ± 0.00085**
Clad -100°C	-0.34%	-0.61%	-0.84%
Moderator -100°C			
Fuel +100°C	1.14387 ± 0.00102	1.06659 ± 0.00092	0.99528 ± 0.00104
Clad = 618K	-0.42%	-0.92%	-0.93%
Moderator = 584K			
Fuel -100°C	1.14445 ± 0.00102	1.06547 ± 0.00097	0.99205 ± 0.00093
Clad = 618K	-0.37%	-1.03%	-1.25%
Moderator = 584K			
Fuel = 1040K	1.14326 ± 0.00103	1.06501 ± 0.00090	0.99131 ± 0.00081

Clad +50°C Moderator +50°C	-0.47%	-1.07%	-1.33%
Fuel = 1040K	**1.14563 ± 0.00092**	1.06860 ± 0.00087	0.99554 ± 0.00083
Clad -50°C Moderator -50°C	-0.26%	-0.74%	-0.91%
Basis Case	1.14866 ± 0.00101	1.07652 ± 0.00097	1.00465 ± 0.00087
Power 100% Conc. Boron = 0 ppm	-0.4195%	-0.9356%	-1.1158%

Table 15: Results for boron variations

	Enrichment 3.0 wt%		
	10 GWd/MTU	20 GWd/MTU	30 GWd/MTU
1000 ppm	**1.04148 ± 0.00088**	**0.95768 ± 0.00087**	**0.88678 ± 0.00078**
500 ppm	1.03765 ± 0.00089	0.95078 ± 0.00093	0.87714 ± 0.00082
Basis, 0 ppm	1.03525 ± 0.00081	0.94421 ± 0.00064	0.86440 ± 0.00049
	Enrichment 3.6 wt%		
	10 GWd/MTU	20 GWd/MTU	30 GWd/MTU
1000 ppm	**1.08878 ± 0.00106**	**1.00632 ± 0.00084**	**0.93789 ± 0.00096**
500 ppm	1.08819 ± 0.00103	1.00466 ± 0.00086	0.93094 ± 0.00084
Basis, 0 ppm	1.08578 ± 0.00077	1.00068 ± 0.00068	0.92120 ± 0.00058
	Enrichment 4.5 wt%		
	10 GWd/MTU	20 GWd/MTU	30 GWd/MTU
1000 ppm	**1.14837 ± 0.00109**	**1.07148 ± 0.00092**	**1.00111 ± 0.00090**
500 ppm	1.14574 ± 0.00090	1.06957 ± 0.00089	0.99732 ± 0.00082
Basis, 0 ppm	1.14482 ± 0.00091	1.06607 ± 0.00071	0.99371 ± 0.00074

As stated above, the fuel elements to be stored may have been exposed to a great variety of operational conditions. Besides the specific power and the operational history, there are other important parameters to be taken into account: average fuel temperature, average temperature of the moderator and boron concentration.

In general, the k_{ef}, varies with the average fuel temperature. This behaviour is expected, since an increase in the fuel temperature causes an increase in the *Doppler* broadening and, therefore, an increased absorption of the ^{238}U resonance, resulting in a spectral hardening, and in an increase in the conversion ^{238}U (plutonium conversion).

Therefore, it is recommended that a reasonable method is used to determine an upper limit for the effective average fuel temperature.

With regard to the moderator, the k_{ef} increases with the moderator temperature, this effect is due to the loss of moderation, since the moderator density decreases when temperature is increased, giving rise to the hardening of the neutron flux. However, the mean average of the moderator is well known and

presents little variation throughout the reactor operation, and therefore, a reasonable estimation of an upper limit can be obtained.

With regard to the boron concentration, it is observed that the k_{ef} increases with the boron concentration during the burnup process, once again, due to the spectrum hardening, caused by the absorption of thermal neutrons in the boron. The burnup of the fuel element is smaller, causing a greater k_{ef}. However, with greater enrichments, the boron concentrations become increasingly larger at the beginning of the cycle, and as such, it will be necessary to carry out calculations with average boron concentrations, sufficient to restrict all sorts of burnup fuel elements.

In the methodology developed, in the isotope analysis, the following parameters have been taken as base values: as average fuel temperature, 1040K, as average moderator temperature, 586K, corresponding to a specification of 313°C, as boron concentration of 1000 *ppm* (assuming that an average concentration of 1000 *ppm* of boron throughout a cycle is considered conservative). The burnup conditions for the isotopic calculation can be seen in Table 16.

**Table 16: Burnup conditions for the isotopic calculation**

| Parameter	
Average moderator temperature	586 *K* (313 °C)
Average fuel temperature	1040 *K* (767 °C)
Temperature of the sheath	618 *K* (345 °C)
Density of the moderator	0.7052 g/cc
Boron concentration on the moderator	1000 *ppm*

VII. SCALE BURNUP PARAMETERS

Following the methodology, SCALE parameters were analyzed in order to compare with previous works using SAS2H sequence on SCALE5.1. For these calculations a burnup of 39.95 GWd/TU was evaluated for a fresh fuel enrichment of 3.7 wt% on U-235.

Figure 7 shows an isometric view of the PWR simulated in KENO-VI, while Figure 8 depicts an axial view of the reactor with its fuel pins and guide tubes configuration, both obtained with KENO3D visualization tool. Figure 9 shows a 2D plot obtained with NEWT, along with the computational mesh.
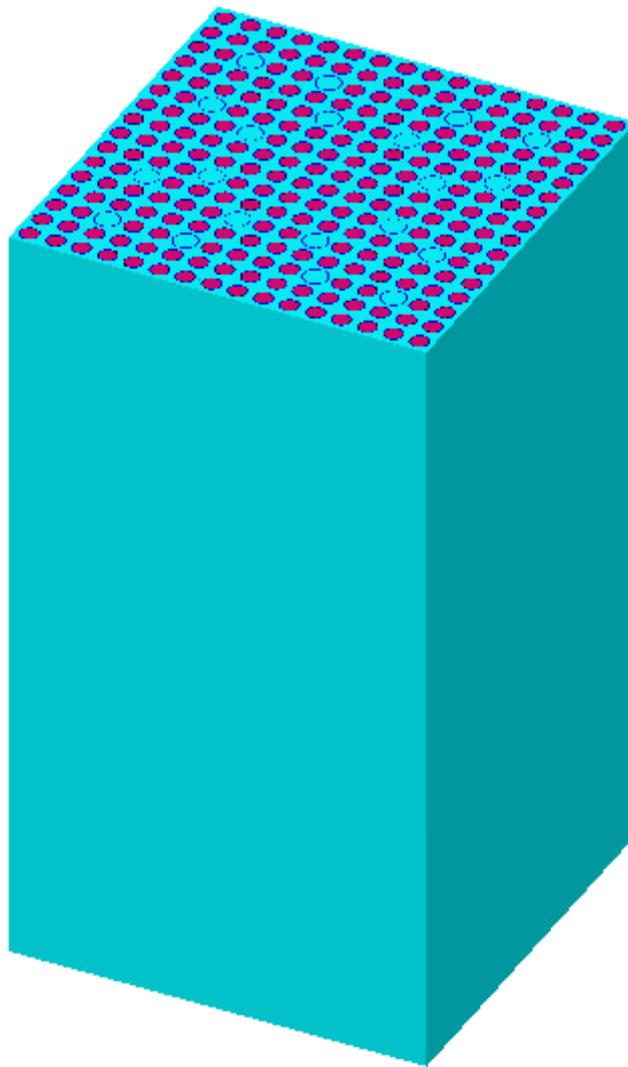
Figure 7: Full PWR fuel element on KENO3D
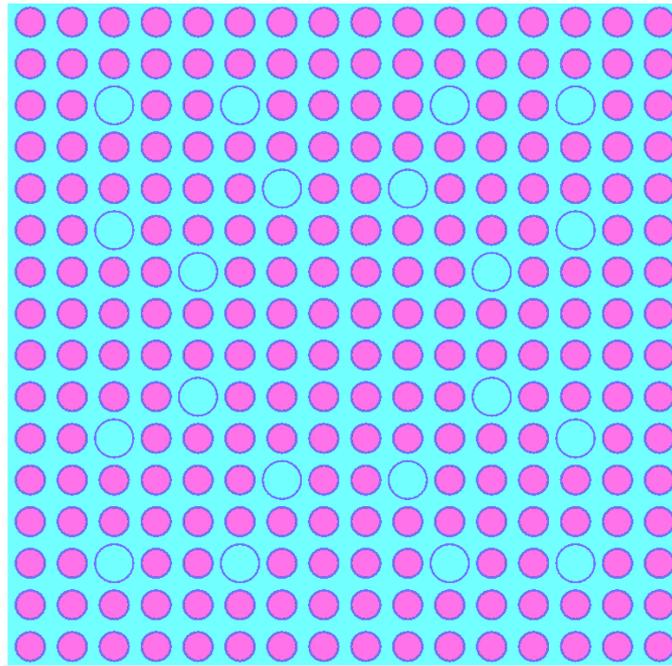
Figure 8: Top view of the PWR fuel element on KENO3D
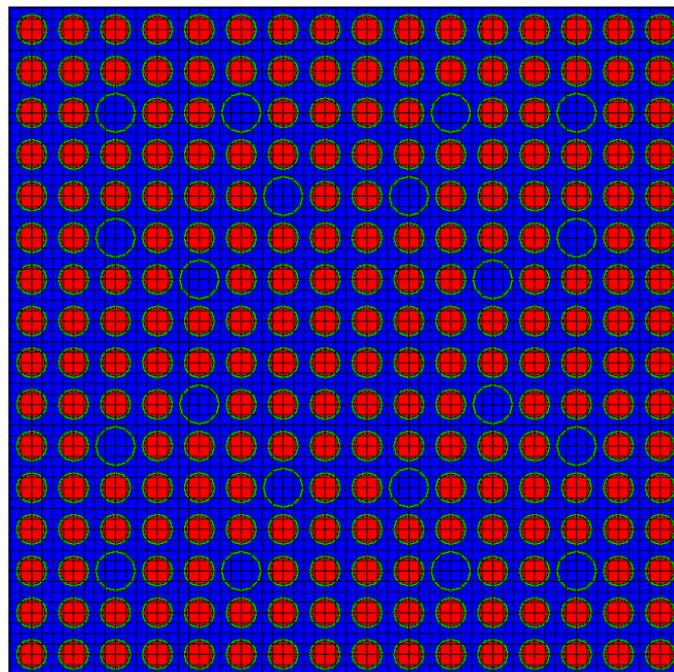
Figure 9: NEWT 2D plot of the PWR fuel element

Following the burnup calculations, the isotopic concentrations for the nuclides on Table 19 are collected and used for the criticality analysis on the spent fuel pool. Figure 9 and Figure 10 show the reference cell of the spent fuel storage pool
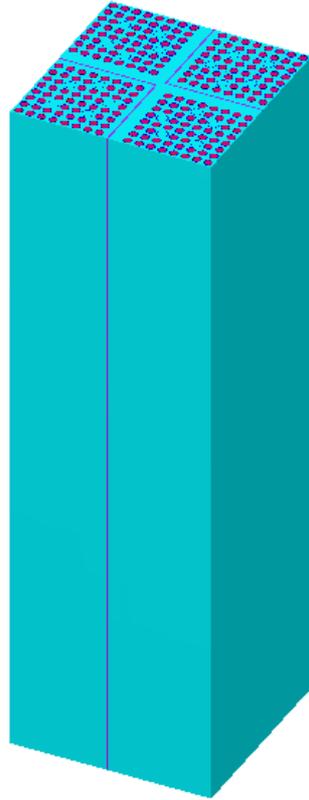
Figure 10: Reference cell of the spent fuel storage pool
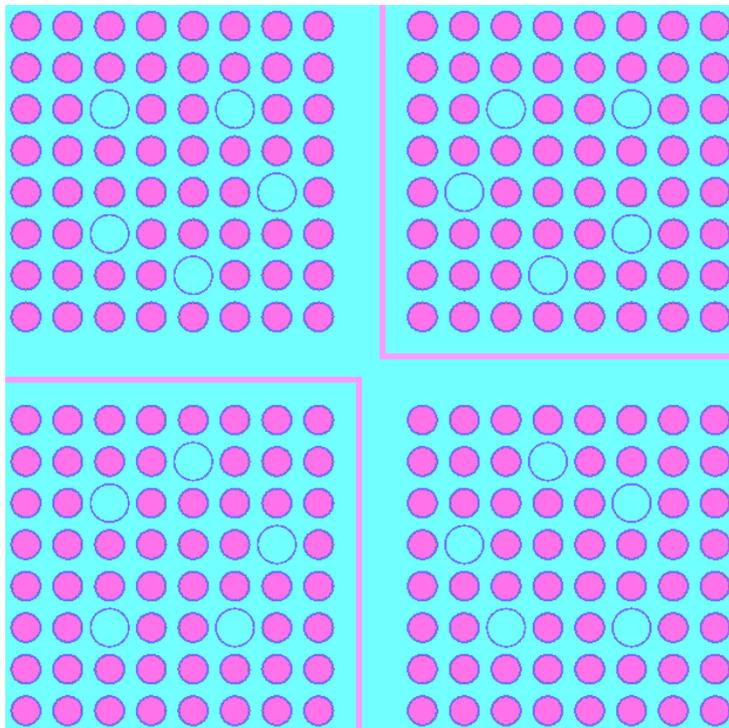
Figure 11: Axial view of the reference cell of the spent fuel storage pool

Some TRITON parameter blocks for burnup were modified   so to evaluate their influence over the burnup calculations:

VII.1   ADDNUX parameter:

Adds to all fuel materials trace quantities (1.0E–20 atoms/b-cm) of a set of nuclides that have been determined to be important in the characterization of spent fuel.

TRITON provides user control of the set of nuclides added to a fuel material through the *parm=(addnux=N)* control parameter, where N is an integer value. For N = 0, no nuclides are added, which is generally a very poor approximation and should only be used when the ramifications are fully understood. For N = 1, a bare minimum set of 15 nuclides (actinides) are added; this will generate improved number density estimates for actinides in low-burnup fuels but will not update cross sections for fission products of primary importance. Again, use of this option is discouraged unless it addresses special modeling needs. For N = 2, the default setting for the TRITON depletion sequences, 94 nuclides are added. N = 3 and N = 4 add 230 and 388 nuclides, respectively; this much detail is generally not needed for depletion calculations unless one wishes to closely estimate k_{eff} near the end of life. At such high burnups, these nuclides have little effect on the system spectrum, but taken as a whole, they do contribute to the total system reactivity.

Table 17 through Table 21 list the set of nuclides added in trace quantities for each value of *addnux*.

Table 17: ADDNUX=1 (15 additional nuclides are added)

	^{234}U	^{235}U	^{236}U	^{238}U	^{237}Np	^{238}Pu	^{239}Pu
^{240}Pu	^{241}Pu	^{242}Pu	^{241}Am	^{242}Am	^{243}Am	^{242}Cm	^{243}Cm

Table 18: ADDNUX=-2 (49 additional nuclides for a total of 64)

^{1}H	^{10}B	^{11}B	^{14}N	^{16}O	^{83}Kr	^{93}Nb	^{94}Zr
^{95}Mo	^{99}Tc	^{103}Rh	^{105}Rh	^{106}Ru	^{109}Ag	^{126}Sn	^{135}I
^{131}Xe	^{135}Xe	^{133}Cs	^{134}Cs	^{135}Cs	^{137}Cs	^{143}Pr	^{144}Ce
^{143}Nd	^{145}Nd	^{146}Nd	^{147}Nd	^{147}Pm	^{148}Pm	^{149}Pm	^{148}Nd
^{147}Sm	^{149}Sm	^{150}Sm	^{151}Sm	^{152}Sm	^{151}Eu	^{153}Eu	^{154}Eu
^{155}Eu	^{152}Gd	^{154}Gd	^{155}Gd	^{156}Gd	^{157}Gd	^{158}Gd	^{160}Gd
^{244}Cm							

Table 19: ADDNUX=2 (30 additional nuclides for a total of 94)

^{91}Zr	^{93}Zr	^{95}Zr	^{96}Zr	^{95}Nb	^{97}Mo	^{98}Mo	^{99}Mo
^{100}Mo	^{101}Ru	^{102}Ru	^{103}Ru	^{104}Ru	^{105}Pd	^{107}Pd	^{108}Pd
^{113}Cd	^{115}In	^{127}I	^{129}I	^{133}Xe	^{139}La	^{140}Ba	^{141}Ce

^{142}Ce	^{143}Ce	^{141}Pr	^{144}Nd	^{153}Sm	^{156}Eu	

Table 20: ADDNUX=3 (136 additional nuclides for a total of 230)

^{72}Ge	^{73}Ge	^{74}Ge	^{76}Ge	^{75}As	^{79}Br	^{76}Se	^{77}Se
^{78}Se	^{80}Se	^{82}Se	^{81}Br	^{80}Kr	^{82}Kr	^{84}Kr	^{85}Kr
^{86}Kr	^{85}Rb	^{86}Rb	^{87}Rb	^{84}Sr	^{86}Sr	^{87}Sr	^{88}Sr
^{89}Sr	^{90}Sr	^{89}Y	^{90}Y	^{91}Y	^{90}Zr	^{92}Zr	^{92}Mo
^{94}Mo	^{96}Mo	^{94}Nb	^{96}Ru	^{98}Ru	^{99}Ru	^{100}Ru	^{105}Ru
^{102}Pd	^{104}Pd	^{106}Pd	^{110}Pd	^{107}Ag	^{111}Ag	^{106}Cd	^{108}Cd
^{110}Cd	^{111}Cd	^{112}Cd	^{114}Cd	^{115m}Cd	^{116}Cd	^{140}Ce	^{113}In
^{140}La	^{112}Sn	^{114}Sn	^{115}Sn	^{116}Sn	^{117}Sn	^{118}Sn	^{119}Sn
^{120}Sn	^{122}Sn	^{123}Sn	^{124}Sn	^{125}Sn	^{121}Sb	^{123}Sb	^{124}Sb
^{125}Sb	^{126}Sb	^{120}Te	^{122}Te	^{123}Te	^{124}Te	^{125}Te	^{126}Te
^{127m}Te	^{128}Te	^{129m}Te	^{130}Te	^{132}Te	^{130}I	^{131}I	^{124}Xe
^{126}Xe	^{128}Xe	^{129}Xe	^{130}Xe	^{132}Xe	^{134}Xe	^{136}Xe	^{134}Ba
^{135}Ba	^{136}Ba	^{137}Ba	^{138}Ba	^{136}Cs	^{142}Pr	^{142}Nd	^{150}Nd
^{151}Pm	^{144}Sm	^{148}Sm	^{154}Sm	^{152}Eu	^{157}Eu	^{232}U	^{233}U
^{159}Tb	^{160}Tb	^{160}Dy	^{161}Dy	^{162}Dy	^{163}Dy	^{164}Dy	^{165}Ho
^{166}Er	^{167}Er	^{175}Lu	^{176}Lu	^{181}Ta	^{182}W	^{183}W	^{184}W
^{186}W	^{185}Re	^{187}Re	^{197}Au	^{231}Pa	^{233}Pa	^{230}Th	^{232}Th

Table 21: ADDNUX=4 (158 additional nuclides for a total of 388)

^{2}H	^{3}H	^{3}He	^{4}He	^{6}Li	^{7}Li	^{7}Be	^{9}Be
^{15}N	^{17}O	^{19}F	^{23}Na	^{24}Mg	^{25}Mg	^{26}Mg	^{27}Al
^{28}Si	^{29}Si	^{30}Si	^{31}P	^{32}S	^{33}S	^{34}S	^{36}S
^{35}Cl	^{37}Cl	^{36}Ar	^{38}Ar	^{40}Ar	^{39}K	^{40}K	^{41}K
^{40}Ca	^{42}Ca	^{43}Ca	^{44}Ca	^{46}Ca	^{48}Ca	^{45}Sc	^{46}Ti
^{47}Ti	^{48}Ti	^{49}Ti	^{50}Ti	^{50}Cr	^{52}Cr	^{53}Cr	^{54}Cr
^{55}Mn	^{54}Fe	^{56}Fe	^{57}Fe	^{58}Fe	^{58}Co	^{58m}Co	^{59}Co
^{58}Ni	^{59}Ni	^{60}Ni	^{61}Ni	^{62}Ni	^{64}Ni	^{63}Cu	^{65}Cu
^{70}Ge	^{69}Ga	^{71}Ga	^{74}As	^{74}Se	^{79}Se	^{78}Kr	^{110m}Ag
^{113}Sn	^{123}Xe	^{130}Ba	^{132}Ba	^{133}Ba	^{136}Ce	^{138}Ce	^{139}Ce
^{138}La	^{148m}Pm	^{153}Gd	^{156}Dy	^{158}Dy	^{166m}Ho	^{162}Er	^{164}Er
^{168}Er	^{170}Er	^{174}Hf	^{176}Hf	^{177}Hf	^{178}Hf	^{179}Hf	^{180}Hf
^{182}Ta	^{191}Ir	^{193}Ir	^{196}Hg	^{198}Hg	^{199}Hg	^{200}Hg	^{201}Hg
^{202}Hg	^{204}Hg	^{204}Pb	^{206}Pb	^{207}Pb	^{208}Pb	^{209}Bi	^{223}Ra
^{224}Ra	^{225}Ra	^{225}Ac	^{226}Ac	^{227}Ac	^{226}Ra	^{227}Th	^{228}Th
^{229}Th	^{233}Th	^{234}Th	^{232}Pa	^{235}Np	^{236}Np	^{238}Np	^{239}Np
^{237}U	^{239}U	^{240}U	^{241}U	^{236}Pu	^{237}U	^{243}Pu	^{244}Pu
^{246}Pu	^{242m}Am	^{244}Am	^{244m}Am	^{241}Cm	^{245}Cm	^{246}Cm	^{247}Cm
^{248}Cm	^{249}Cm	^{250}Cm	^{249}Bk	^{250}Bk	^{249}Cf	^{250}Cf	^{251}Cf

^{252}Cf	^{253}Cf	^{254}Cf	^{253}Es	^{254}Es	^{255}Es		

Burnup calculations were performed for all of the six possible cases. Results in terms of k_{eff} are shown in Table 22 and are plotted on Figure 11.

Table 22: k_{ef} variation with ADDNUX parameters

Step Number	addnux=0	addnux=1	addnux=-2	addnux=2	addnux=3	addnux=4
0	1.24661	1.24635	1.24556	1.24556	1.24612	1.24612
1	1.22804	1.23621	1.18385	1.18373	1.18291	1.18247
2	1.18933	1.20412	1.13843	1.13699	1.13717	1.13669
3	1.14683	1.17426	1.09819	1.09554	1.09383	1.09267
4	1.09668	1.14574	1.06155	1.05727	1.05522	1.05488
5	1.03823	1.11888	1.02733	1.02068	1.02057	1.01947
6	0.97279	1.09105	0.99525	0.98837	0.98814	0.98633
7	0.89764	1.06465	0.9652	0.95765	0.95558	0.95444
8	0.81068	1.04089	0.93724	0.93013	0.92863	0.92663
9	0.71169	1.01571	0.91046	0.90215	0.90167	0.90022

There is one step for each cross-section processing on the burnup calculations on TRITON. Because three libraries for each burnup cycle were created, nine calculation steps are performed. Step number zero is the first cross-section processing and is performed at the burnup time equal zero, i.e. beginning of life.
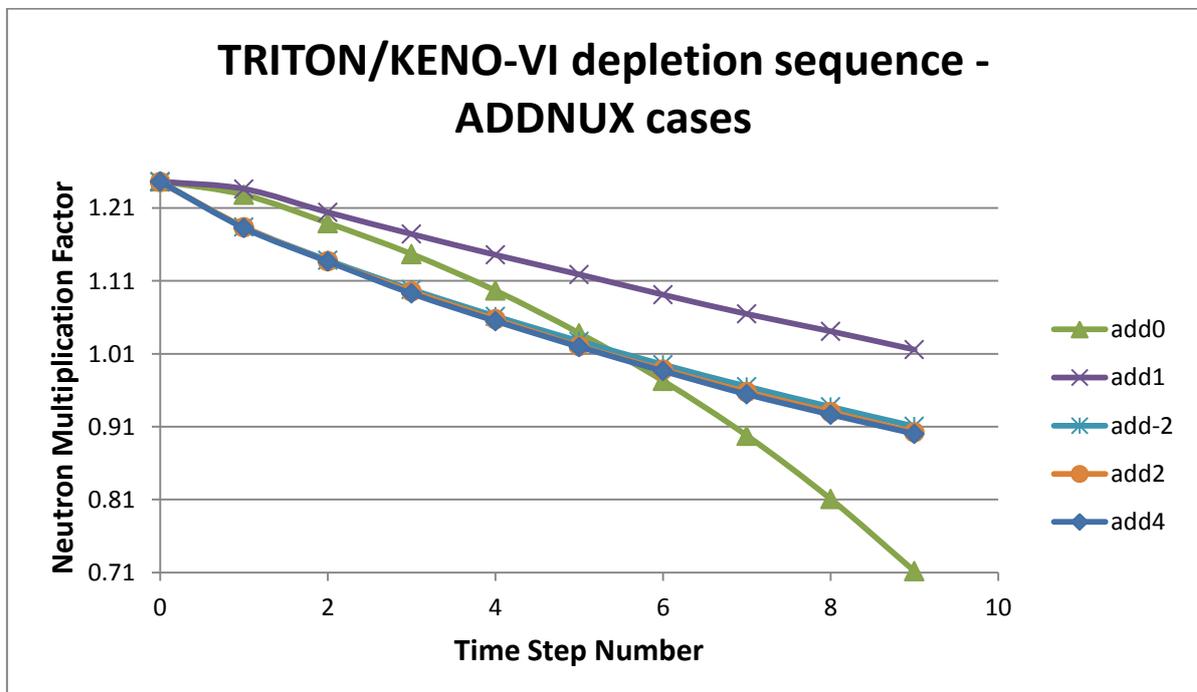
Figure 12: k_{ef} variation with ADDNUX parameters

VII.2   TIMETABLE Block

This block allows modification of material properties such as temperature and density during a depletion calculation. In this specific case, soluble boron dissolution on the moderator is to be taken into account. At each time step, the boron concentration in the moderator is modified by a multiplication factor and TRITON applies linear interpolation between each pair (step, density multiplier). The user-specified density multipliers were obtained from previous works using the SAS2H burnup sequence on SCALE5.1, which also worked as motivation and comparison basis of such calculations. Table 23 provides the data used for specifying the applied density multipliers along with the time steps, in days, on which these factors were applied. On Figure 12 the concentration values on TRITON and SAS2H for the isotope b-10 are plotted.

Table 23: Boron letdown timetable applied to the calculations

Time Step Number	Time Step [Days]	Density Multiplier
0	0	1.75
1	61	1.6
2	183	1
3	304	0.4
4	441	1.6
5	563	1
6	684	0.4
7	821	1.6
8	943	1
9	1064	0.4
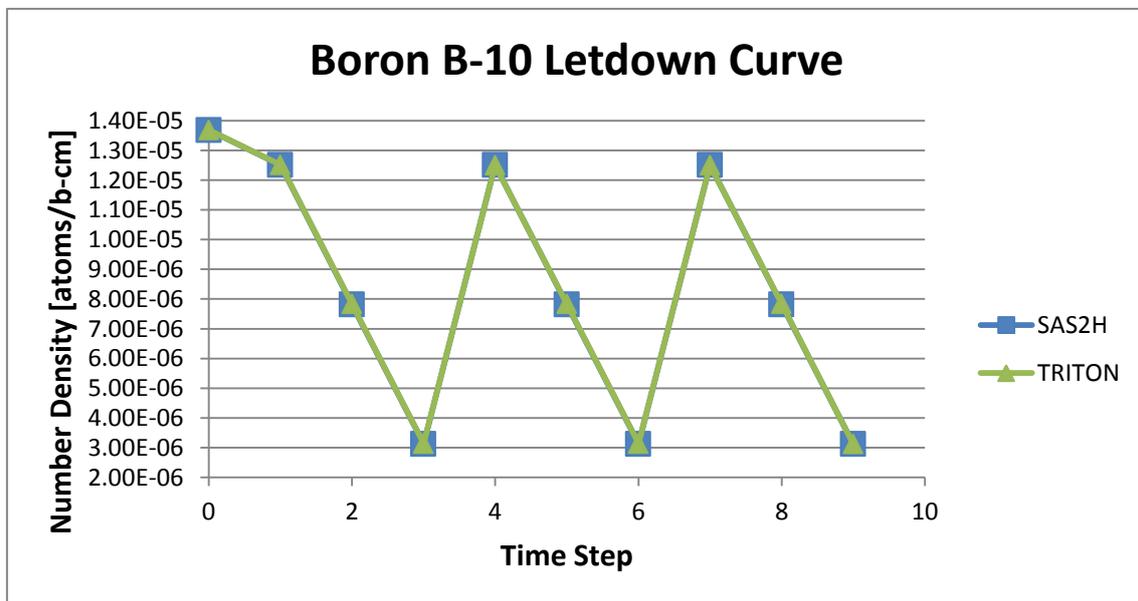
Figure 13: Boron letdown curve applied to the calculations

As expected the curves from TRITON and SAS2H are identical. One must be aware that

VII.3 TIMETABLE and ADDNUX Analysis

Taking into account both of the previous analyses, calculations using the boron letdown curve from SAS2H and the ADDNUX cases were carried out. The results for KENO-VI and NEWT are shown on Table 25 and Table 26, and plotted on Figure 13 and Figure 15. On these charts, *addnux=N* stands for the ADDNUX set used (N=0, 1, -2, 2, 3, 4), while sas2h are the results for the case run by SAS2H on SCALE5.1. Because SAS2H automatically adds a set of nuclides in the neutron transport calculations, as depicted on Table 24, another set of nuclides was manually included on TRITON calculations, using *addnux=0* and specified as part of the fuel composition at trace quantities (1.0E–20 atoms/b-cm) so as to match the nuclides included by SAS2H. This case is labeled *atoms* and follows in Table 25, Table 26, Figure 14 and Figure 15 as well.

Table 24: List of fuel nuclides automatically included by SAS2H in neutron transport calculation

Xe-135	Pu-240	Cs-133	Pu-241	U-234	Pu-242
U-235	Am-241	U-236	Am-242m	U-238	Am-243
Np-237	Cm-242	Pu-238	Cm-243	Pu-239	Cm-244

Table 25: k_{ef} variation for ADDNUX cases with boron letdown with KENO-VI

Step	sas2h	addnux=0	addnux=1	addnux=-2	addnux=2	addnux=3	addnux=4	atoms
0	1.1738	1.16905	1.17	1.16907	1.16907	1.17047	1.16866	1.16962
1	1.149	1.1645	1.17689	1.13067	1.12833	1.12796	1.12747	1.14345
2	1.1792	1.18909	1.20726	1.14006	1.13732	1.13795	1.13617	1.16992
3	1.2114	1.22896	1.23898	1.15292	1.14785	1.14958	1.1464	1.19704
4	1.0645	1.01975	1.09035	1.01509	1.01084	1.00992	1.00848	1.06028
5	1.0945	1.03994	1.11966	1.02866	1.02303	1.02192	1.02063	1.0845
6	1.1281	1.07478	1.15391	1.04473	1.03701	1.03648	1.03553	1.11572
7	0.9854	0.81506	1.0112	0.91985	0.91545	0.91482	0.91374	0.98316
8	1.0171	0.81209	1.04321	0.93923	0.93099	0.93061	0.92713	1.01352
9	1.0518	0.81646	1.07722	0.95846	0.94783	0.94733	0.94534	1.04447

Table 26: k_{ef} variation for ADDNUX cases with boron letdown with NEWT

| Step	sas2h	addnux=0	addnux=1	addnux=-2	addnux=2	addnux=3	addnux=4	atoms
0	1.1738	1.16903226	1.16903226	1.16898883	1.16898883	1.16902082	1.16902082	1.16902506
1	1.149	1.16327576	1.17622196	1.12856301	1.12762808	1.12748105	1.12729322	1.14318741
2	1.1792	1.18880893	1.20647047	1.13968718	1.13748727	1.137396	1.13635958	1.16994937
3	1.2114	1.22948941	1.23824729	1.15279661	1.14921763	1.14891842	1.1473277	1.19782099
4	1.0645	1.01992009	1.08855119	1.01381778	1.00978741	1.00938198	1.00779951	1.05896905
5	1.0945	1.03918419	1.11959408	1.02794796	1.02262386	1.02192783	1.02001667	1.08560343
6	1.1281	1.07277066	1.15380981	1.04502006	1.03827685	1.03731281	1.03519194	1.11611967
7	0.9854	0.81501232	1.00898428	0.92131243	0.9147382	0.91360215	0.91212162	0.98319424
8	1.0171	0.81165139	1.042596	0.93882438	0.93093432	0.92963771	0.92782854	1.01239853
9	1.0518	0.8155127	1.07828142	0.95801608	0.94863821	0.94716444	0.94522407	1.04440638
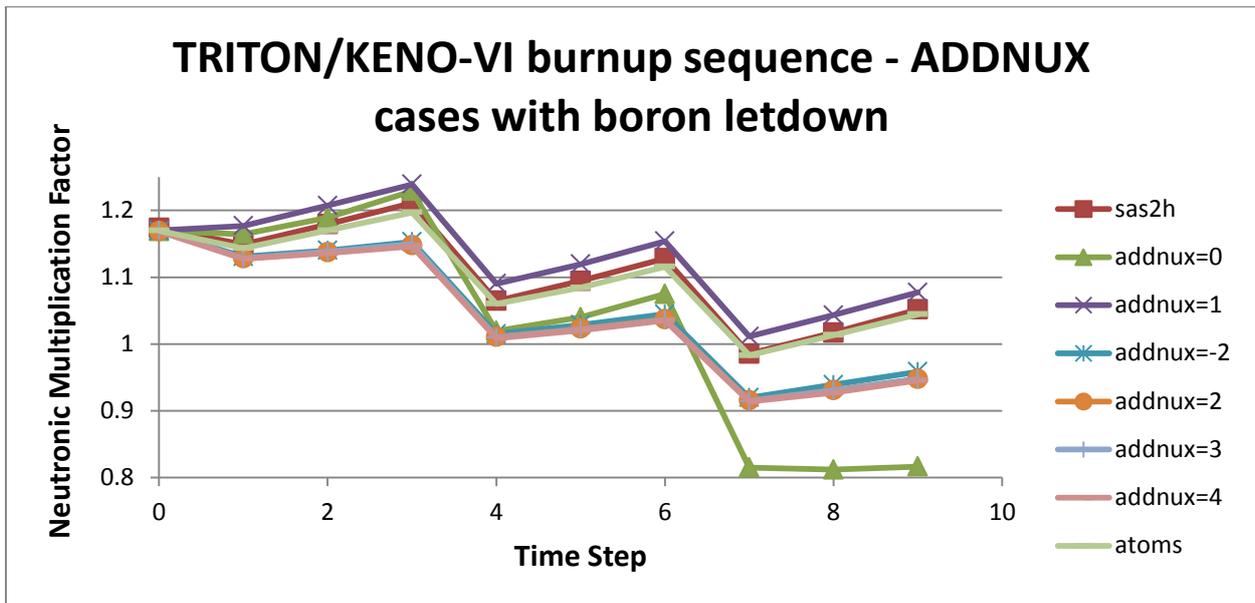
Figure 14: k_{ef} **variation for ADDNUX cases with boron letdown using KENO-VI**
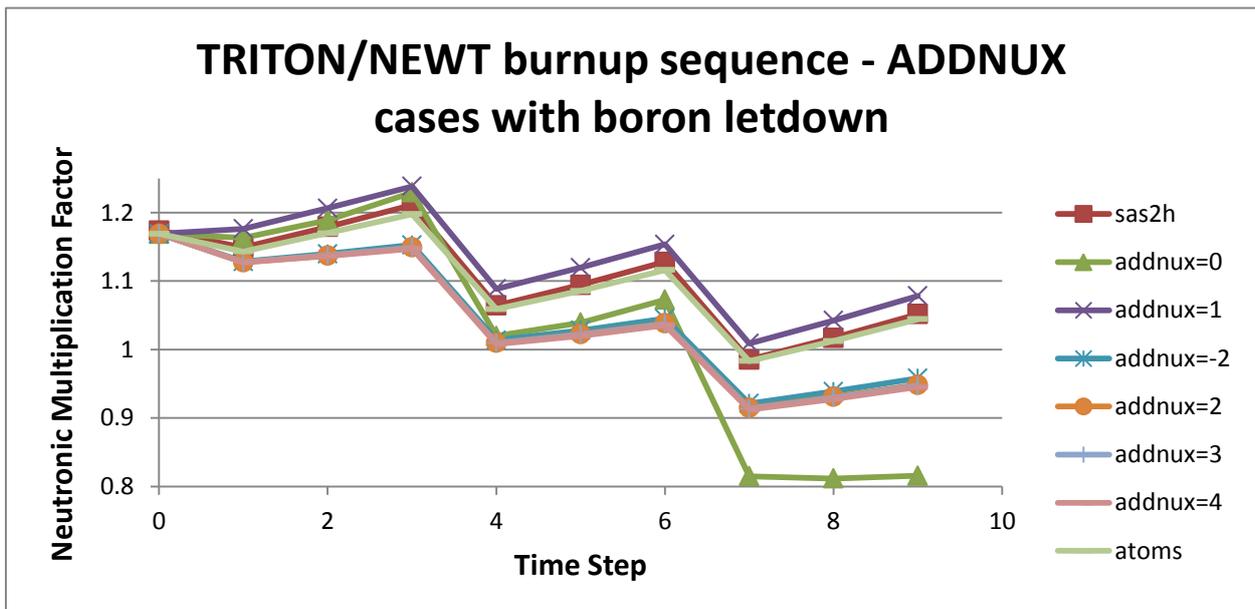
Figure 15: k_{ef} **variation for ADDNUX cases with boron letdown using NEWT**

The inventory obtained from these calculations, after all the burnup cycles, is collected with OPUS and used on a follow-up criticality analysis by CSAS6 performed for the region II of the spent fuel storage pool. Results for TRITON/KENO-VI and TRITON/NEWT depletion are shown on Table 26 and plotted on Figure 16 and Figure 17

Table 27: Criticality analysis for the region II of the spent fuel storage pool

Case	K$_{ef}$ (KENO-VI)	K$_{ef}$ (NEWT)

addnux=0	0.76012 ± 0.00068	0.75991 ± 0.00089
addnux=1	0.86618 ± 0.00095	0.86448 ± 0.00089
addnux=-2	0.89210 ± 0.00085	0.89096 ± 0.00079
addnux=2	0.89265 ± 0.00080	0.89062 ± 0.00078
addnux=3	0.89205 ± 0.00083	0.89306 ± 0.00080
addnux=4	0.89324 ± 0.00083	0.89174 ± 0.00079
atoms	0.87517 ± 0.00080	0.87365 ± 0.00078
sas2h	0.86955 ± 0.00076	0.86955 ± 0.00076
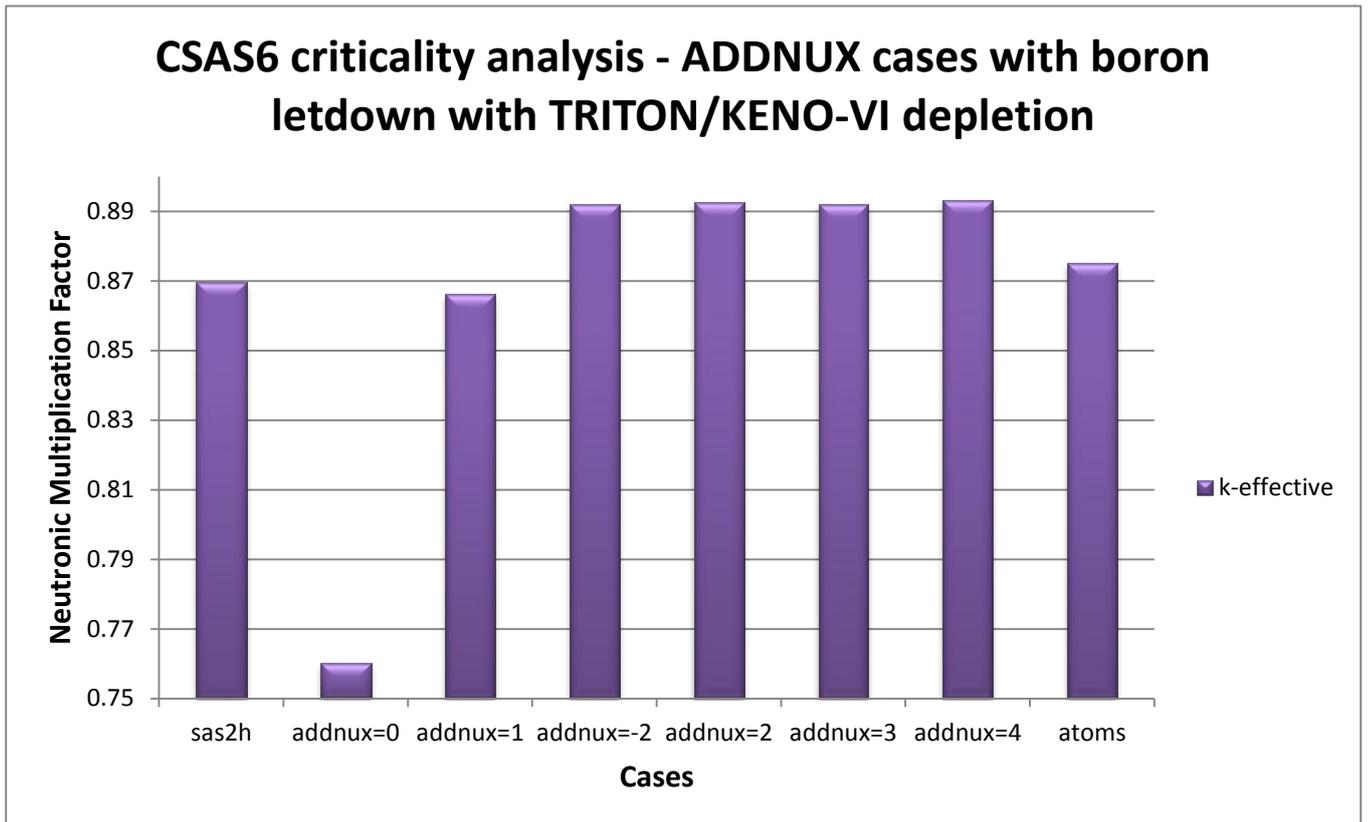
Figure 16: Criticality analysis for the region II of the spent fuel storage pool (TRITON/KENO-VI depletion sequence)
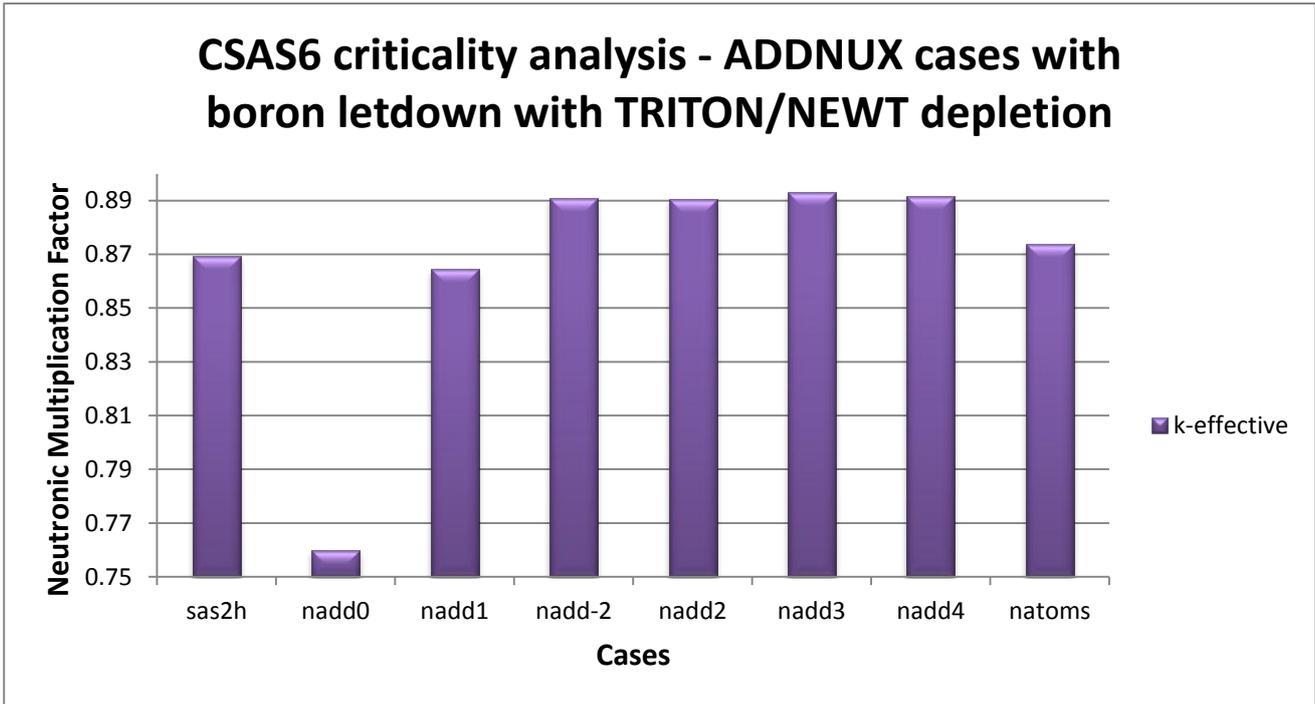
Figure 17: Criticality analysis for the region II of the spent fuel storage pool (TRITON/NEWT depletion sequence)

Results on this study show that, although SAS2H depletion gives a good approximation of the isotopic concentration, the inclusion of the fission products presents a more conservative k_{eff}. For that reason, the parameter *ADDNUX* was set to ADDNUX=2 and will be held through further analysis.

VII.4 CENTRM Data

SCALE default parameters are suitable for most of the problems. Nevertheless, some CENTRM parameters were modified in order to evaluate how they affect the system:

- ISN: CENTRM order of angular quadrature
- ISCT: CENTRM Pn order of scattering
- ISCTI: CENTRM inelastic Pn order of scattering

The cases are as follows:

Case 1: isn=4 isct=1 iscti=1 (Default)

Case *2*: isn=4 isct=2 iscti=1

Case *3*: isn=4 isct=3 iscti=1

Case *4*: isn=6 isct=3 iscti=1

Case *5*: isn=6 isct=3 iscti=2

Case *6*: isn=6 isct=3 iscti=3

Case *7*: isn=6 isct=3 iscti=2, 238-groups ENDF/B-VII library

The depletion calculations were carried out using the TRITON/KENO-VI code. The results are shown in Table 27 and plotted in Figure 15.

Table 28: k_{ef} variation with CENTRM parameters

Step	C01	C02	C03	C04	C05	C06	C07
0	1.24454	1.24516	1.24374	1.24593	1.24695	1.24695	1.25344
1	1.18208	1.18175	1.18164	1.1838	1.18268	1.18268	1.18775
2	1.13496	1.1343	1.13577	1.13705	1.13721	1.13721	1.14302
3	1.09268	1.09428	1.09461	1.09577	1.09451	1.09451	1.09609
4	1.05641	1.05577	1.05351	1.05444	1.05592	1.05592	1.0603
5	1.02035	1.0201	1.02038	1.02062	1.02105	1.02105	1.02475
6	0.98674	0.98715	0.98733	0.98891	0.98849	0.98849	0.99159
7	0.95828	0.95804	0.95685	0.95709	0.95721	0.95721	0.96016
8	0.92819	0.9278	0.92954	0.92863	0.92964	0.92964	0.93091
9	0.90078	0.90297	0.90183	0.90059	0.9019	0.9019	0.90348
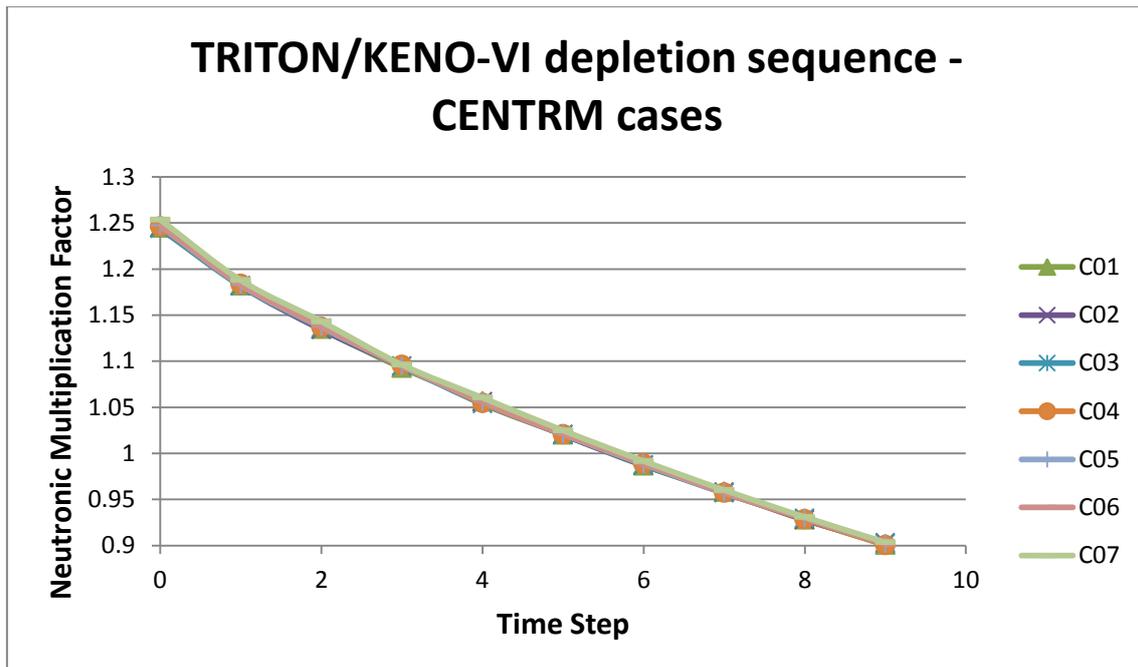
Figure 18: k_{ef} variation with CENTRM parameters

The results for this calculations show little difference between the cases. CENTRM default parameters were used for all the following calculations in this work.

VIII. AXIAL BURNUP CREDIT METHODOLOGY

VIII.1 Introduction

When a fuel element is introduced in a PWR reactor, the quasi-sine wave flux will carry out a greater burnup of the element in the central section than in the ends. The quasi-sinusoidal form of the flux is a consequence of many factors, such as the leakages at the extremes and the concentration of fission products in the central part of the element.

When a uniform axial isotopic distribution is assumed, the most reactive region of the element is the mean axial plane. The neutron flux is smaller in the extremes than in the core, since the leakages are greater at the element edges. However, the most reactive area of the spent fuel is at the ends, where there is equilibrium between the reactivity due to low burnup and the increase of neutron loss in the fuel element end.

At low average burnups, of around 20 GWd/TU, the maximum rate of fissions occurs in the axial core or nearby. The approximation to the uniform axial burnup uniformly distributes the burnup throughout the length of the element. Thus, the decrease of reactivity in the central section is artificially compensated by an increase at the ends, and a more reactive configuration, and as such, is more conservative than the real profile results.

However, as the average burnup increases, the equilibrium obtained between the central section and the ends disappears, and therefore the hypothesis of uniform burnup is no longer conservative. This is the **End Effect**, an increase in reactivity at the ends of a fuel element caused by a decrease in the neutron flux, due to leakages.

The *End Effect* gives a characteristic axial burnup distribution, with a *plateau* in the central area of the element and two slopes with lower burnup at the ends

In order to obtain a numerical approximation of the axial isotopic variation, it is necessary to discretize the profile of axial burnup by areas, assuming a constant burnup in each area. The mean point of each area is defined as a node.

The isotopic concentrations can be estimated using just one decay calculation with SAS2H for each axial node burnup. The number and size of the required axial zones to appropriately deal with the axial burnup variations must be determined by a parametric study, which is always a function of the database of the actual existing profiles. For the present methodology, as a result of the data available, it was considered that each profile could be divided into 32 nodes.

In figure 5 a typical profile of the axial burnup in a PWR fuel element with 32 nodes can be seen, where node **B1** represents the lower end of the element and node **B32** the upper end.

As can be observed in Figure 16, the burnup of the lower nodes is slightly superior to the burnup of the lower nodes (usually with the exception of the first inferior node, which usually has lower burnup due to the axial profile of the neutron flux). This is because the water that is exposed to each node presents varying densities. The lower end reacts with colder water (greater density), resulting in greater reactivity, and, therefore, the burnup is greater than at the upper end. Water reaches the upper area of the fuel at a higher temperature (lower density) due to the warming produced by the fission heat, which involves lower reactivity and, therefore, a lower burnup.
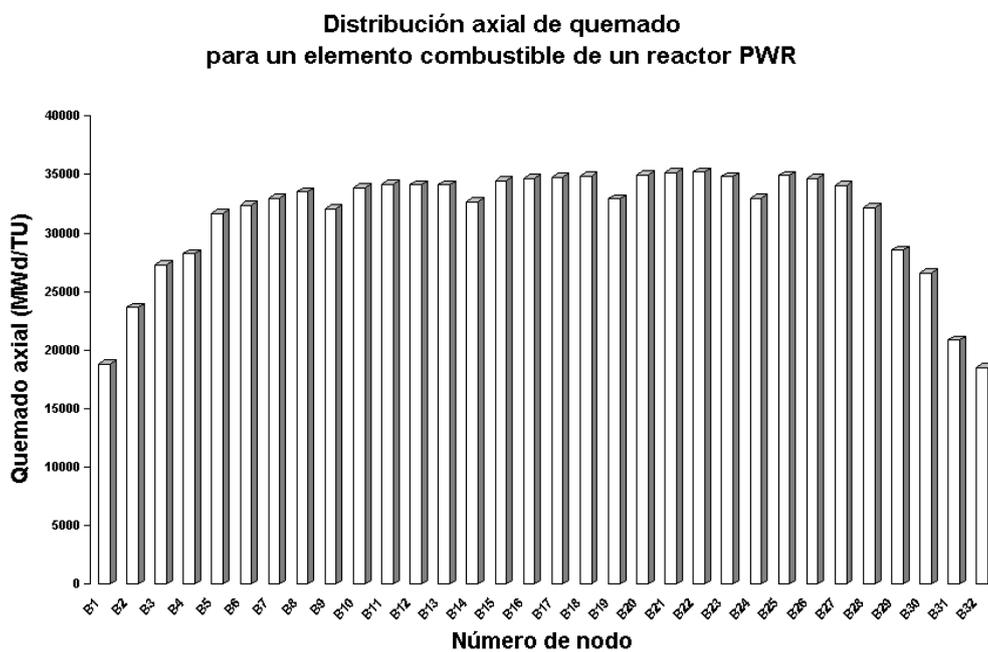
Figure 19: Axial burnup distribution for a fuel element in a PWR reactor

When a uniform average axial burnup of a fuel element is assumed, infinity is imposed on the axial direction. That is, under this hypothesis, the k_∞, effective product constant, is calculated, without taking into account the leakages, that is, with infinite geometry in X, Y and Z directions.

However, as stated above, it is possible that this approximation is not conservative, since the effect of the axial burnup distribution can cause the k_{ef} to be greater than the k_∞ calculated with a uniform burnup. Under these circumstances, the geometric model that will be used will not be axially infinite, but real in the Z direction, when using a water reflector of 30 cm. both above the surface and beneath it. The outcome of considering different geometric configurations suggests that the average burnup hypothesis is

conservative up to a certain level of average burnup and, that, for greater burnups, the axial distribution effect correction would be more conservative.

VIII.2 Objective of the methodology

The objective of the present methodology is to secure a , which, being more conservative than the uniform burnup profile for high burnups and high enrichments can be modelled according to the actual physical burnup. This profile will be used in the design of the Equivalent Reactivity Curve (ERC) for the discharge of fuel elements in region II of the spent fuel pool at the PWR power plant.

First of all, a validation of the code system SCALE6.1 is conducted, in order to obtain the upper subcritical limit (USL), which will be the limit acquired by the effective product constant in safe conditions.

Since the fuel elements of region II are spent fuel elements, the burnup of the element will be modelled using its isotopic content, previously simulated in a case with TRITON (ORIGEN-S).

In order to obtain the most conservative hypothetical profile, it will be necessary to check that for the same burnup and enrichment conditions, any real profile is less critical than the stated profile. For this, different samples of real profiles will be extracted and simulated, to obtain the normalised real profile with the most critical burnup, and to compare this with the hypothetical profiles.

Once the most conservative profile is calculated, the calculations for acquiring the loading curve will provide the criterion for determining whether a fuel element should be stored in region I or in region II, using the value of the previously obtained, upper subcritical limit (*USL*). Figure 17 that follows shows an outline of the process carried out.
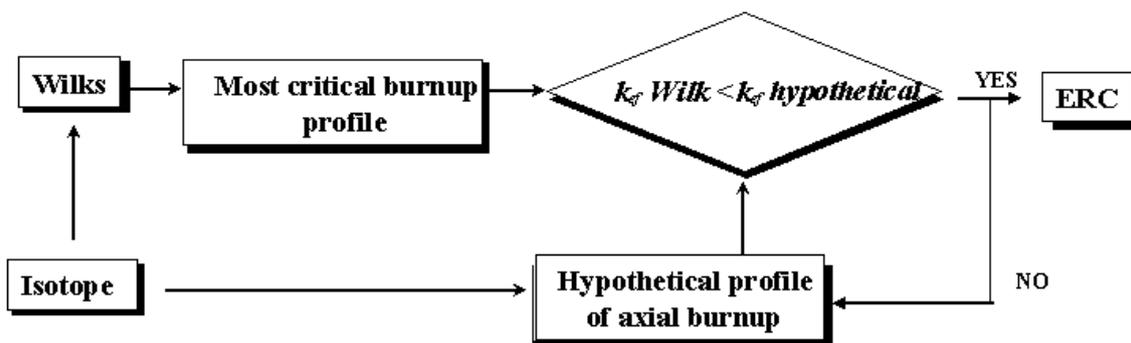

Figure 20: Outline representing the most important points developed in the methodology.

VIII.3 Axial profile correction

WILKS' METHODOLOGY
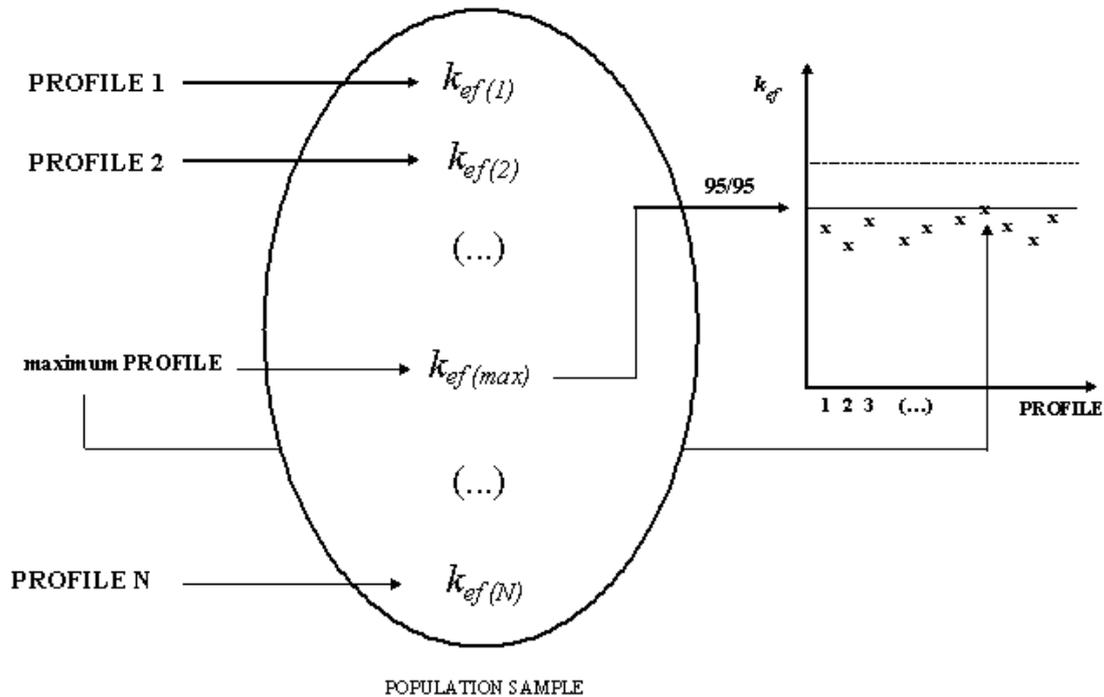
Figure 21: Description of Wilks methodology in order to obtain the most critical burnup profile

Thus, since the axial burnup profile notably influences the criticality calculations, it will be necessary to obtain a hypothetical profile, which is able to provide a conservative representation of a fuel element of average burnup and specific enrichment.

For this, and taking into account that the application is made for region II of the PWR spent fuel elements pool, the database of axial profiles is available, supplied by the PWR, and reconstructed by the processing computer. From it, the axial profiles have been grouped accordingly to the initial enrichment of the fuel element (1.9%, 2.5%, 3.3%, 3.5%, 3.7%, 3.85%, 3.95%, 4.35% and 4.5%). Following this, they are grouped in burnup ranks, independent from the initial enrichment. The maximum width of each interval has been fixed at 2 GWd/TU, in order to obtain the maximum number of profiles per rank, and so that the previously mentioned profiles, once normalised can be representative of it. That is, by stating the rank [39,41] GWd/TU centred around the mean value of 40 GWd/TU, it can be assumed that the normalised axial profile corresponding to a fuel element with average burnup, for instance of 39.5 GWd/TU is very similar to that of another fuel element with an average burnup within the same rank.

In addition, it must also be taken into account that, as the average burnup increases, the normalised burnup at the ends will also increase, with the result that if we were to choose higher ranks for the study of the average burnup (>40 GWd/TU), the k_{ef} would be sensibly lower. However, there is a commitment to

apply the methodology, which, on one hand, uses the maximum number of profiles, and on the other hand the minimum possible burnup interval band. The width of the established band satisfies both criteria.

In order to analyse different profiles with average burnup, for instance, of 40 GWd/TU, a burnup band between 39 and 41 GWd/TU is determined. Then, the corresponding burnup of each axial node ($B_{i,j}$) is divided by the average burnup relative to that profile (B_j), and is multiplied by the average burnup under study ($\overline{B}^{analysis}$),

$$B_{i,j}^{normalised} = \frac{B_{i,j}}{B_j} . \overline{B}^{analysis}$$

i, axial node,   *j*, number of profile.

In contrast with the criticality analyses which take the fresh fuel elements as a starting point, burnup credit needs to consider the operational history of the fuel element, including the axial burnup distribution.

VIII.4 Criticality analysis of real profiles

Wilks [12] establishes that the maximum value of an average sample of a magnitude measured from a sample of *N* elements is the single-sided upper tolerance limit, with a γ probability and a level of reliability α, of the values of this magnitude. A diagram of Wilks' methodology is shown in the Figure 18.

According to Wilks, for non-parametric tolerance limits (only at one end), such that with probability γ, at least α per one of the population does not exceed the maximum sampling value, a sample of the following size must be taken:

$$N = \frac{ln(1-\gamma)}{ln\ \alpha} \approx 58$$

For γ equal to 0.95 and α equal to 0.95, the sampling size must be approximately 58. For each rank of average burnups of Wilks' sampling, the maximum possible number of profiles has been chosen, so that the sampling sizes are always around this value.

For our example, the magnitude measured using Wilks' method, is the value of the k_{ef} of a normalised real burnup profiles sampling. If we obtain for different average burnup ranks [27,29], [33,35], and [39,41] a GWd/TU with average burnups of 28, 34 and 40 GWd/TU, respectively for each rank, a sample of *n=58* fuel elements, the maximum value among all the profiles of the k_{ef} sample would be the upper tolerance limit, *UL₁*, which secures a probability and a level of reliability at 95/95. These burnup ranks have been chosen because they are of interest when studying the effect of the axial profiles.

44

The normalised real profile, that has an upper tolerance limit UL_1 in the value of the k_{ef} for an average burnup analysis is defined as the **most critical axial burnup profile**.
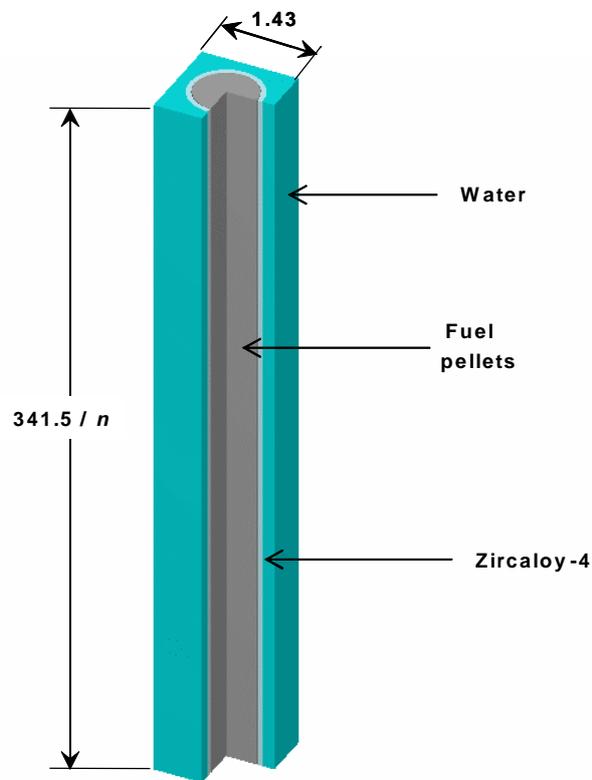
Figure 22: Model with KENO3D of a burnup node n_i of the fuel pellet. The number of burnup nodes (n) is 32.

An axial burnup node of the fuel pellet where the different materials, the maximum active length of the node and the pellet *passage* are shown in Figure 19 whereas in Figure 20, the stack of the different axial nodes to form the complete model of the fuel pellet is given. For all the models, 32 axial burnup nodes have been used. The active length of the pellet was calculated after considering the nominal length of the pellet plus the maximum core fabrication tolerance (*341.5* cm.).
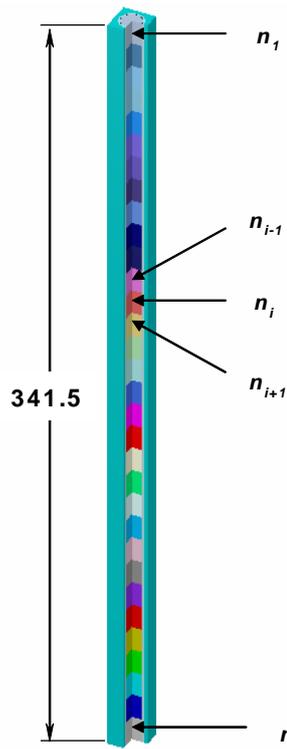
Figure 23: Model with KENO3D of a fuel pellet of n nodes of *341.5* cm. of maximum active length. The number of burnup nodes is 32.

Due to the unfeasibility of obtaining a sample of 58 fuel elements with the same average burnup, at least 58 axial profiles were extracted from the database within the burnup rank with a maximum band of 2 GWd/TU, for all the given enrichments.

This part of the work is still to be implemented, with the use of available profiles from the PWR in question. The simplified process to obtain a conservative axial burnup profile would be as follows:
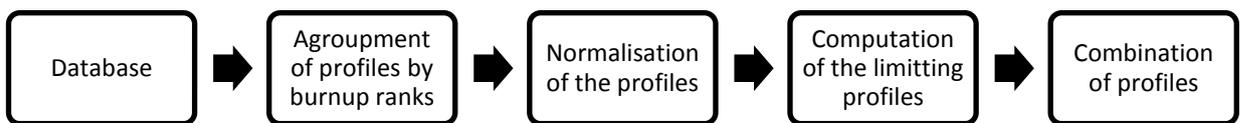
The chart depicts the basic steps to find the bounding axial burnup profiles from real profiles as described above.

IX. CONCLUSIONS AND FUTURE WORKS

A burnup credit methodology under development has been studied. Once a conservative bias and its uncertainty is established, the USL was determined, which is the safety limit for a spent fuel storage pool. The recommendations for giving burnup credit to a certain system, specifies that axial burnup is to be considered at high burnup levels. This is a step still in progress and should be analyzed nevertheless. With the USL and axial profile burnup analysis, it will be possible to obtain the loading curve which determines whether a fuel element will be stored in the region I or II.

Using the codes TRITON/KENO-VI and CSAS6, different types of PWR operational histories were analyzed. The codes are vastly validated with experimental data and give reliable and accurate nuclear data for this criticality analysis. This study allowed obtaining the closest to reality operational history that remains conservative in terms of criticality.

NRC research efforts are currently directed toward developing the technical basis and information for revising ISG8R2 to allow credit for fission products. The goal is to develop and establish a technically sound validation approach (both depletion and criticality) for SNF criticality safety evaluations based on best-available data and methods, to demonstrate the approach and applicability, and to provide reference bias results. Specifically, for isotopic validation, the planned approach is to use a best estimate Monte Carlo-based method to determine burnup-dependent reactivity bias and bias uncertainty in isotopic predictions via comparisons of isotopic composition predictions and measured isotopic compositions from destructive radiochemical assay, utilizing as much assay data as is available [13].

Future works must include the axial burnup evaluation with nodes discretization with real burnup profiles. Finding the most conservative simulated axial profile for which all of the real profiles are considered safe is a needed step on the progress of this work. Also, assuming ISG8R3 will contemplate the full burnup credit recommendations, the issuance of this guide will allow more details for giving validation and consequent use for this methodology.

X. REFERENCES

1. U.S. Nuclear Regulatory Commission Interim Staff Guidance 8 – Revision 2, *'Burnup Credit in the Criticality Safety Analyses of PWR Spent Fuel in Transport and Storage Casks'*. Nuclear Regulatory Commission. 2002

2. J.C. Wagner, M.D. DeHart, *'Review of Axial Burnup Distribution Considerations for Burnup Credit Calculations'*. Oak Ridge National Laboratory. March 2000.

3. A. Machiels, *'Burnup Credit Methodology - Spent Nuclear Fuel Transportation Applications'*. Electric Power Research Institute (EPRI). Report. 2010.

4. C.V. Parks, et. al., *'Full Burnup Credit in Transport and Storage Casks: Benefits and Implementation'*. American Nuclear Society 2006 International High-Level Radioactive Waste Management Conference. April 30 – May 4, 2006. Las Vegas, Nevada.

5. 10 CFR 50.68, *'Criticality Accident Requirements'*. U.S. Nuclear Regulatory Commission

6. NRC memorandum from L. I. Kopp to T. Collins, *'Guidance on the Regulatory Requirements for Criticality Safety Analysis of the Fuel Storage at Light-Water Reactor Plants'*, U. S. Nuclear Regulatory Commission. Agosto 1998.

7. C.V. Parks. *'Recommendations for PWR Storage and Transportation Casks That Use Burnup Credit'*. 2003 International High-Level Radioactive Waste Management Conference, "Progress Through Cooperation". March 30 – April 2, 2003. Las Vegas, Nevada.

8. M.D. DeHart, S.M. Bowman, 'Reactor Physics Methods and Analysis Capabilities in SCALE'. Oak Ridge National Laboratory, Nuclear Science and Technology Division. September, 2010.

9. Oak Ridge National Laboratory. 'SCALE6.1 Electronic Manual'. ORNL/TM. June 2011..

10. J. J. Lichtenwalter, S. M. Bowman, M. D. DeHart, C. M. Hopper *'Criticality Benchmark Guide for Light-Water Reactor Fuel in Transportation and Storage* Packages', NUREG/CR-6361, ORNL/TM-13211. Oak Ridge National Laboratory, March 1997.

11. UNE 73-501-92. *'Requisitos de Criticidad para el Diseño de Bastidores de Almacenamiento en Piscinas de Combustible'*.

12. M. D. DeHart, S. M. Bowman, *'Validation of the SCALE Broad Structure 44-Group ENDF/B-V Cross-Section Library for Use in Criticality Safety Analyses'*, NUREG/CR-6102, ORNL/TM-12460.

13. I.C. Gauld, *'Strategies for Application of Isotopic Uncertainties in Burnup Credit'*. Prepared for Division of Systems Analysis and Regulatory Effectiveness Office of Nuclear Regulatory Research. U.S. Nuclear Regulatory Commission

14. S. S. Wilks, 'Collected papers: Contributions to mathematical statistics', Ed. John Wiley, 1967.

15. C.V. Parks, et. al., *'Development of Technical Basis for Burnup Credit Regulatory Guidance in the United States'*. 16th International Symposium on the Packaging and Transport of Radioactive Materials, London, 3 - 8 October 2010.